The Interdisciplinary Sciences Journal

TCABSE-J

ISSN: 2583-2557 Volume 1 Issue 4 Oct 5th, 2022.

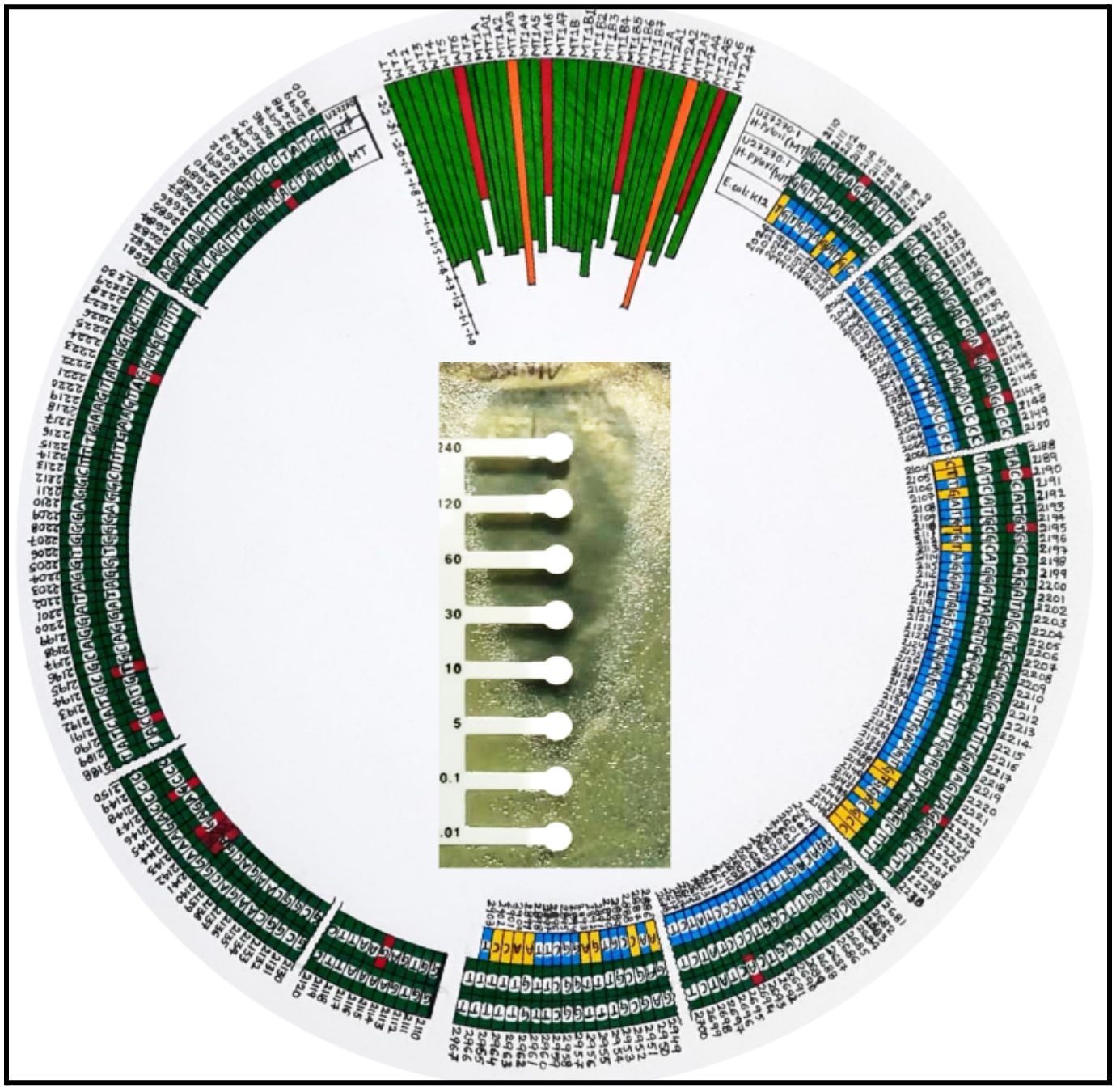

The Center for Advanced-Applied Biological Sciences & Entrepreneurship (TCABS-E). Rajamahendravaram. India.

Table of Contents

TCABSE-J Research Article
ISSN: 2583- 2557, *Volume 1, Issue 4, pp1-8. 2022.*

TCABSE-J
Interdisciplinary Sciences Journal

Evaluation of genotoxicity caused by the carcinogenic benzo[a]pyrene, a common ingredient of Indian tobacco chew, using a bacterial gene expression model.

[1, 2]Kishan Maru, [1, 3]Niharikha Mukala, [1]Madhumita Aggunna and [1, 4]Ravikiran S. Yedidi*

[1]The Center for Advanced-Applied Biological Sciences & Entrepreneurship (TCABS-E), Visakhapatnam 530016, AP; [2]Department of Biochemistry, [3]Department of Biotechnology, [4]Department of Zoology, Andhra University, Visakhapatnam 530003, AP. (*Correspondence to RSY: tcabse.india@gmail.com)

Tobacco consumption (chewing and smoking) mainly causes many forms of cancer, such as Lung cancer, kidney cancer, cancer of the larynx, head, neck, bladder, esophagus, pancreas, liver etc. Tobacco products contain various carcinogens such as Polycyclic aromatic hydrocarbons (PAHs), *N*-nitrosamines, aromatic amines, 1,3-butadiene, benzene, aldehydes, and ethylene oxide are the most important carcinogens. Cytochrome P450 enzymes are important in metabolizing PAHs to epoxide intermediates, which are further converted to diol epoxides, the ultimate carcinogens. CYP-1A1/1B1 enzymes catalyze activation of pro-carcinogenic and metabolic activation of PAH. CYP-1A1/1B1 gene expression is induced by PAH and polyhalogenated hydrocarbons through aryl-hydrocarbon receptors. In this study, we used bacterial gene expression as a model system to demonstrate the lethal effects of B[*a*]P. Our results show that the gene expression in bacteria is indeed affected by B[*a*]P. Based on our results, we extrapolate that B[*a*]P can cause cancer by changing the gene expression levels in humans in a similar way that was observed in this study.

Keywords: Tobacco chew, B[a]P, Carcinogen, cyp450, Cancer, PAH, smoking.

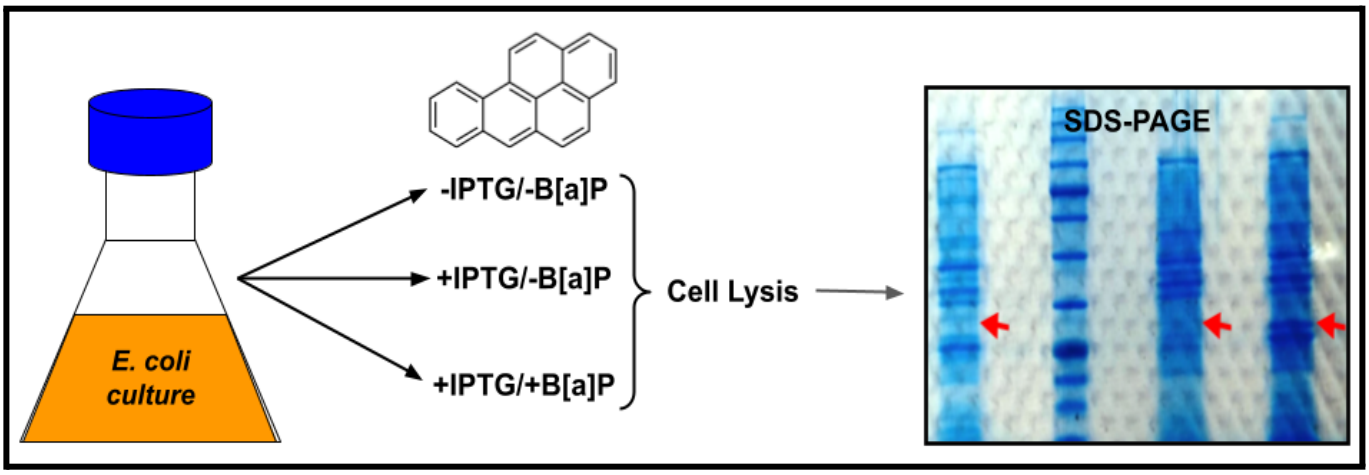

Figure 1. Overview of bacterial gene expression analysis in the presence and absence of B[a]P followed by SDS-PAGE analysis.

Citation: Maru, K., Mukala, N., Aggunna, M. and Yedidi, R.S. (2022). Evaluation of genotoxicity caused by the carcinogenic benzo[a]pyrene, a common ingredient of Indian tobacco chew, using a bacterial gene expression model. *TCABSE-J*, Vol. 1, Issue 4:1-8. Epub: Oct5th, 2022.

CC BY NC ND

TCABSE-J Research Article
ISSN: 2583- 2557, *Volume 1, Issue 4, pp1-8. 2022.*

The condition in which cells divide uncontrollably and spread into surrounding tissues called CANCER. There are more than 100 types of cancers known (according to the organ or tissue affected). There are various types of cancer; Carcinoma, Sarcoma, and Leukemia. Proto-oncogenes, tumor suppressor genes, and DNA repair genes are responsible for genetic changes in the cell, which leads to cancer. Sometimes, these genetic changes are called “drivers" of cancer. Proto-oncogenes participate in normal cell growth and division. Tumor suppressor genes also control cell growth and division. DNA repair genes participate in fixing damaged DNA.Additional mutations and changes in their chromosomes develop in these genes of a cell, like duplications and deletions of chromosome parts. *Carcinoma* is a cancer of the epithelial cell, which covers the surfaces of the body. *Sarcomas* are the type of cancers formed in many tissues like soft and fibrous tissues, bones and muscle, fat, blood vessels, lymph vessels etc. Cancers that form in the blood are called *leukemias.* These cancers are not solid tumors. Instead, large numbers of abnormal leukocytes increased in the blood and bone marrow, with decreased normal blood cells.

According to the National Cancer Institute, our lifestyle choices are known to increase your risk of cancer. Women should not drink or smoke more than one time per day and men should not drink or smoke twice per day,frequent exposure to sun or continuous blistering sunburns, obesity, and unsafe sex can cause cancer. People who smoke or chew tobacco products like cigarettes and tobacco chew mainly cause lung cancer and mouth cancer. LUNG CANCER: Lung cancer is a type of cancer that forms in the lungs. Globally, lung cancer is the main cause of cancer deaths. Smokers have the greatest risk of lung cancer, even non-smokers can also cause lung cancer. The risk of lung cancer increases with the number of cigarettes we've smoked in a particular period of time. If we quit smoking, even after smoking for many years, we can reduce your chances of developing lung cancer. In the earliest stages, lung cancer doesn't show any signs and symptoms. Symptoms of lung cancer are seen when the disease is advanced. Signs and symptoms of lung cancer: Non-stop cough, Coughing up blood, in small amounts, Shortness of breath, Chest pain, Hoarseness, Losing weight, Bone pain, Headache.

Smoking causes mainly lung cancers - both in active and passive smokers. Doctors believe smoking damages the cells that line the lungs and causes lung cancer. Inhaling cigarette smoke immediately changes the lung tissue. Initially our body may be able to repair this damage. After each repeated exposure, normal cells lining our lungs are increasingly damaged. Types of lung cancer: Based on the observation of lung cancer cells under the microscope, doctors divide lung cancer into two major types. Based on the type of lung cancer, treatment is decided. The two types of lung cancer: Small cell lung cancer: Small cell lung cancer is less prevalent than non-small cell lung cancer and nearly exclusively affects heavy smokers. Non-small cell lung cancer: Non-small cell lung cancer (NSCLC) is a catch-all name for a variety of lung malignancies.Non-small cell lung cancers include squamous cell carcinoma, adenocarcinoma, and large cell carcinoma.

Tobacco refers to a group of plants of the *Solanaceae* family's *Nicotiana* genus, as well as any product derived from their cured leaves. Tobacco comes in over 70 different species, although *N. tabacum* is the most prevalent commercial crop. In some areas, the more potent variety *N. rustica* is also used. Tobacco includes both nicotine and harmala alkaloids, which are extremely addictive stimulants. Tobacco use is linked to a variety of severe diseases, including those affecting the heart, liver, and lungs, as well as a variety of malignancies. Tobacco use was rated the world's single largest avoidable cause of death by the World Health Organization in 2008. Tobacco in the Americas has been reported back to 1400-1000 BC in Mexico. Tobacco has long been grown and used by many native Americans.

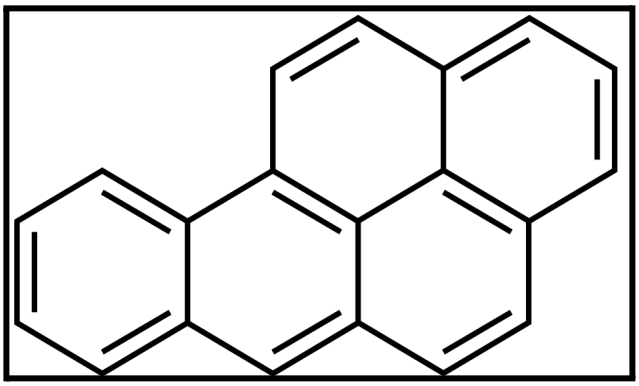

Figure 2. Two-dimensional structure of Benzo[a]Pyrene.

Tobacco was traditionally carried in pouches by people from the Northeast Woodlands tribes as a commonly acceptable trade item. It was smoked for social purposes as well as for ceremonial purposes, such as to seal a peace treaty or a trade transaction. Tobacco is seen as a gift from the Creator in several Native tribes, with ceremonial tobacco smoke sending one's thoughts and prayers to the Creator. The Tobacco Board of India is headquartered in Guntur, Andhra Pradesh. There are 96,865 tobacco farmers registered in India, with many more unregistered. In 2010, there were 3,120 tobacco product production plants in India. Tobacco production takes up about 0.25 percent of India's cultivated land. The tobacco business has been sponsored by the Indian government since 1947. Tamil Nadu, Andhra Pradesh, Punjab, Bihar, Mysore, and West Bengal each have a tobacco research center, with the central research institute in West Bengal. In genetics, several tobacco plants have been employed as model organisms. Tobacco BY-2 cells, which are generated from the *N. tabacum* cultivar 'Bright Yellow-2,' are one of the most important plant cytology research tools. Tobacco has laid the framework for modern agricultural biotechnology by pioneering callus culture research and elucidating the mechanism through which kinetin functions. In 1982, *Agrobacterium tumefaciens* was used to make the first genetically engineered plant, an antibiotic-resistant tobacco plant. This study paved the way for all genetically engineered crops to follow.

CARCINOGENIC METABOLITES IN TOBACCO: The smoke that comes out of a cigarette's mouthpiece is an aerosol with around 1010 particles per milliliter and 4800 chemical components. A glass fiber filter has been used to separate cigarette smoke vapor components from the particle phase in experiments. The vapor phase smoke will account for more than 90% of the total smoke weight. Nitrogen, oxygen, and carbon dioxide are the most common chemicals in the vapor phase. Nitrogen oxides, isoprene, butadiene, benzene, styrene, formaldehyde, acetaldehyde, acrolein, and furan are all highly carcinogenic vapor phase chemicals. At least 3500 chemicals are found in the particulate phase of smoke, with polycyclic aromatic hydrocarbons (PAH), N-nitrosamines, aromatic amines, and metals accounting for the majority of carcinogens. In these models, PAH-containing fractions of the condensate also cause cancers, but the PAH concentrations are too low to explain the carcinogenicity. Other condensate fractions show tumor-promoting and co-carcinogenic properties, enhancing the carcinogenicity of the PAH-containing fractions. The International Agency for Research on Cancer has identified over 60 carcinogens in cigarette smoke for which there is "sufficient evidence for carcinogenicity" in either laboratory animals or people. PAH (10 compounds), aza-arenes (3), N-nitrosamines (8), aromatic amines (4), heterocyclic amines (8), aldehydes (2), volatile hydrocarbons (4), nitro compounds (3), miscellaneous organic compounds (12), metals and other inorganic compounds (12) are among the substances they include (9). Other carcinogens that have not been evaluated by the IARC are also likely to exist. Multiple alkylated and high molecular-weight compounds, for example, have been discovered among the PAHs, although their carcinogenicity has yet to be determined. PAH, aza-arenes, tobacco-specific nitrosamines, e.g. 4-(methylnitrosamino)-1-(3- pyri -dyl)-1-butanone (NNK), 1,3-butadiene, ethylene oxide, nickel, chromium, cadmium, polonium-210,

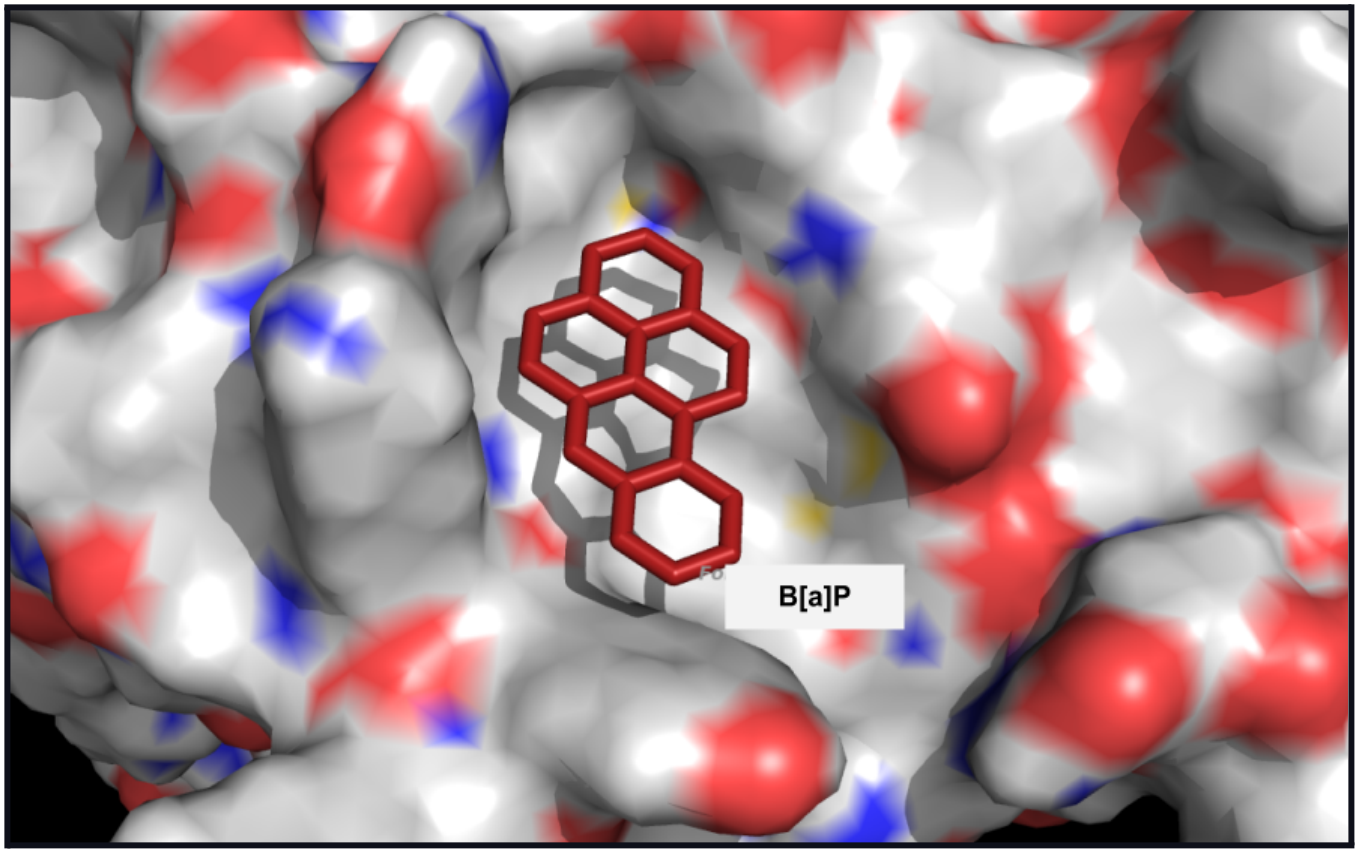

Figure 3. B[a]P docked into the active site of CYP450 1A1.

arsenic, and hydrazine are all known lung carcinogens in cigarette smoke. These chemicals have been found in cigarette smoke and have been shown to cause lung cancers in at least one animal species.

Benzo[a]pyrene (B[a]P) is the most widely investigated of the PAHs, and its capacity to cause lung tumors when administered locally or inhaled has been demonstrated conclusively. When B6C3F1 mice were given B[a]P in their diet, no lung tumors appeared. B[a]P is more carcinogenic than benzofluoranthene or indeno[1,2,3-cd]pyrene in tests of lung tumor production by implantation in rats. The existence of B[a]P in cigarette smoke has been proven by extensive analytical evidence. It has a sales-weighted concentration of roughly 9 ng per cigarette in today's 'full-flavored' cigarettes. The abundance of B[a]P literature tends to draw attention away from other topics. Benzo[a]pyrene (B[a]P) is the most thoroughly researched PAH, and its capacity to cause lung tumors when administered locally or inhaled has been demonstrated conclusively.

Cytochrome P450 enzymes catalyze the addition of an oxygen atom to a carcinogen, enhancing its solubility in water and transforming it to a more easily excretable form. Phase 2 enzymes, which convert the oxygenated carcinogen to a form that is extremely soluble in water, aid this metabolic detoxification process. The organism will be safeguarded to the extent that this process is effective. However, some of the intermediates generated by cytochrome P450 enzymes interacting with carcinogens are extremely reactive, having an electrophilic (electron-deficient) core. DNA adducts can occur when such intermediates or metabolites react with DNA.

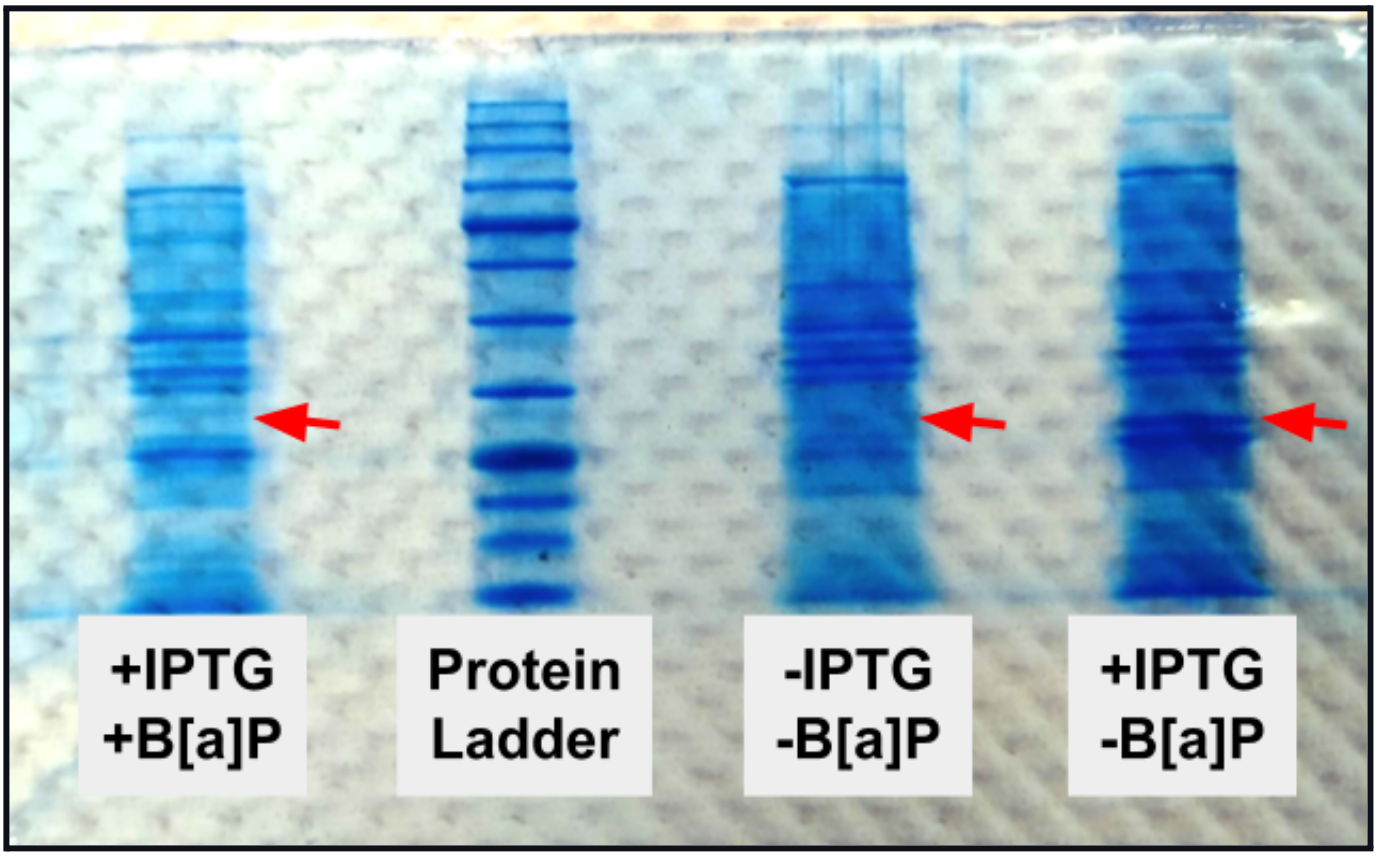

Figure 4. Gene expression analysis of cell lysates SDS-PAGE.

Metabolic activation is the process of converting an unreactive carcinogen into a form that can bind to DNA. Because DNA adducts are crucial to the carcinogenic process, the balance between metabolic activation and detoxification differs among individuals and is expected to alter cancer risk. The majority of carcinogens found in cigarette smoke require metabolic activation.To remove DNA adducts from the genome, complex DNA repair processes have emerged. P450 (CYP) 1A1 is involved in the metabolism of endogenous substrates and medicines, as well as the activation of some poisons and pollutants. CYP1A1 is well-known for its ability to biotransform polycyclic aromatic hydrocarbons into carcinogens, such as benzo[a]pyrene in tobacco smoke.

In this study, we hypothesized that B[a]P may have a direct effect on the gene expression profiles of various organs in humans thus contributing to various cancers. In order to test this hypothesis, we used a bacterial gene expression system in which we examined the protein expression levels qualitatively using SDS-PAGE. Protein expression was performed using an IPTG-inducible system in the presence and absence of B[a]P.

Materials & Methods:

Docking B[a]P into the active site of CYP450-1A1: The procedure was followed from a previously published article [21]. Briefly, the CYP450-1A1 was taken as a receptor and a docking grid was built as shown in Figure 8 into which B[a]P (ligand) was docked to obtain multiple binding poses. Exhaustive sampling was done to obtain multiple binding poses of the ligand

in order to manually verify the appropriate binding orientation using the binding affinity values as a guiding tool. The ligand 3-D structure was imported from a 2-D diagram using ChemSketcher software. The ligand was further energy minimized to avoid any steric clashes or bad contacts before docking into the docking grid built into the active site of the receptor.

Bacterial gene expression:

Preparation of LB Broth: In 100 ml of deionised water,add 2.5grams of LB broth. Autoclave it for 15minutes under 15lbs pressure.
Preparation of LB Agar: Prepare LB-Agar by adding 0.5gm of LB powder and 0.3gm of agar powder in 40ml of deionised water,(for 1 petri plate).Autoclave it for 15 minutes under 15lbs pressure.Let it cool down to luke warm.After it attains room temperature, pour it into petri dishes and let them turn into solid.
Preparation of Ampicillin (50mg/ml): Add 3 mg of ampicillin in 600 ml of deionised water. Store it at -20 ℃ until further use.

Resuspend the *E.coli* cells in vial by adding 0.25ml of LB broth. In 100 ml of deionised water, add 2.5grams of LB powder. Autoclave it for 15-20 minutes under 15lbs pressure. Prepare LB-Agar by adding 0.5gm of LB powder and 0.3gm of agar powder in 40ml of deionised water (for 1 petri plate). Add ampicillin into the LB-agar just before pouring it into the petri plates. Add Ampicillin and LB-agar into petri plates and wait until it solidifies. These plates can either be used immediately after the LB Agar solidifies or for later purposes, the plates must be stored at 4℃. After LB-agar solidifies,streak inoculum in a zig-zag pattern and incubate at 37 ℃ for 24hrs/overnight until colonies appear.

After the colonies appear, *E.coli* colonies are grown in 50ml of LB-broth and incubate it for 2hrs. Take 5 ml LB-broth in three different test tubes labeled as (1) IPTG (Isopropyl ß-D-1-thiogalactopyranoside); (2) IPTG + B[A]P and (3) control (uninduced culture) indicate as BI-Before induction (no IPTG and no B[A]P) and AI (only IPTG, no B[A]P). Incubate these tubes for 2hrs. After incubation, transfer the samples in centrifuge tubes for centrifugation. Place the samples of AI and BI in a centrifuge and run it at 8000 rpm for 10 mins. The supernatant is discarded and the pellet is retained. In these pellets, add 0.1ml of cell lysis buffer and wait for a few minutes(DO NOT VORTEX) to let lysis of the *E.coli* cells to analyze the labile macromolecules of the cells. Boil the AI and BI samples in a water bath for 8-10 mins. Centrifuge AI and BI samples at 8000 rpm for 10mins. Transfer the supernatant to a fresh tube without disturbing the pellet.
SDS-PAGE: Preparation of 12% Separating gel: 30% acrylamide-bisacrylamide -6ml, Deionised water-3ml, 2.5Xtris SDS-buffer -6ml (pH-8.8), 10%APS solution-125ul, TEMED-7.5ul. Preparation of 5% Stacking gel: 30% acrylamide-bisacrylamide-1.3ml, Deionised wat er-5.1ml, 5X tris-SDS buffer (pH-6.8)-1.6ml, 10% APS solution-7.5ul, TEMED-15ul.
SDS-PAGE has two plates .i,e., thick plate and thin plate placed vertically parallel in the plate holder. Take some distilled water and pour it in between the plates to check for any leakage. In case of any leakage, immediately change the plates. After leakage testing, discard the water and pour separating gel in between the plates filling upto half of the space. Wait until it solidifies. Add stacking gel in between the plates, above the solidified separating gel until it fills another half. Place the comb in the top of the stacking gel in between the plates in order to form wells for us to load the samples (protein) later. Wait until the gel gets solidified and remove the comb safely without disturbing the wells. Add the obtained samples of B[A]P, IPTG+B[A]P Sample, Control (no IPTG and no B[A]P) with the help of a micropipette in the well. The entire set is kept into the electrophoresis chamber which has positive and negative electrodes. With the help of a Gel running buffer, which is added inside the chamber, will

help to run entire electrophoresis for 2 hrs. The GEL, after 2 hrs, is taken out carefully from the plates without getting it torn. For staining the gel overnight, Carefully transfer the gel without tearing it, into the gel staining dye. After staining it overnight, now the gel is transferred into the destaining solution overnight so that the extra stain is removed from the gel. After the destaining process, the gel picture is taken.

Results and Discussion:

Binding pose of B[a]P in the active site of CYP-1A1: Among the nine different binding poses obtained, the best pose was selected based on its highest binding affinity as shown in Figure 3. B[a]P (shown as red color stick model) docking pose in the active site cavity of the CYP-1A1 (shown as white surface model). B[a]P being a highly hydrophobic molecule, no hydrogen bonding or electrostatic interactions were seen as expected. All interactions are of hydrophobic nature.

B[a]P decreased bacterial gene expression: Based on the SDS-PAGE analysis, it was found that the bacterial gene expression in the presence of B[a]P is relatively decreased when compared to the control (absence of B[a]P). As shown in Figure 4, the protein levels significantly decreased in the presence of B[a]P. The left most lane shows lack of protein expression in the presence of B[a]P (indicated by the red arrow). The right most lane shows presence of protein expression in the absence of B[a]P (red arrow). The two center lanes are protein molecular weight ladder (center left lane) and negative control (center right lane). The current study focused on the genotoxic effects of B[a]P on the bacterial gene/protein expression. Our studies indicate that in presence of B[a]P, the bacterial gene/protein expression decreased significantly and suggest that a similar effect is possible in humans as well, especially in people that chew and/or smoke tobacco products containing B[a]P.

B[A]P is a carcinogenic agent that causes lung cancer. The bands formed in the Gel of SDS-PAGE shows that B[A]P is affecting the normal expression of protein. Before Induction (BI), where we don't add B[A]P & IPTG no expression is seen and absence of CYP enzymes which metabolizes the Carcinogens and other drugs. After Induction (AI), where IPTG is added and B[A]P is not added to the *E.coli* culture, shows that IPTG helps the gene expression without mutation. As the structure of CYP1A1 and 1B1 with B[A]P is not available in the PDB, we constructed the structure by using the software called autodock tools. To know the exact position of binding of B[A]P to both CYP1A1 & 1B1, we will conduct X-ray diffraction to study the structure of binding of B[A]P in future and that structure can be deposited to the PDB.

Although the metabolites of B[a]P were to be blamed for carcinogenicity in humans, in this study, we did not use a humanized system yet we observed changes in gene expression suggesting that B[a]P by itself or its metabolites may cause the phenotype. Alternatively, we make an assumption that bacterial cells contain homologs of human CYP450 1A1/1A2/1B1. Deeper mechanistic studies are yet to be performed to understand the details in the future.

References

1. Shimada, T., & Fujii-Kuriyama, Y. (2004). Metabolic activation of polycyclic aromatic hydrocarbons to carcinogens by cytochromes P450 1A1 and 1B1. *Cancer science*, *95*(1), 1–6. https://doi.org/10.1111 /j.1349-7006.2004.tb03162.x
2. Pfeifer GP, Denissenko MF, Olivier M, Tretyakova N, Hecht SS, Hainaut P. Tobacco smoke carcinogens, DNA damage and p53 mutations in smoking-associated cancers. Oncogene. 2002 Oct 21;21(48):7435-51. doi: 10.1038/sj.onc.1205803. PMID: 12379884.
3. https://www.mayoclinic.org/diseases-conditions/cancer/symptoms-causes/syc-2037058
4. Rudgley, Richard. "Tobacco: from The Encyclopedia of Psychoactive Substances". *Biopsychiatry*. Little, Brown and Company (1998). Retrieved November 26, 2017.
5. "WHO Report on the global tobacco epidemic, 2008 (foreword and summary)" (PDF). World Health Organization. 2008. p. 8. Archived from the original (PDF) on February 15, 2008. Tobacco is the single most preventable cause of death in the world today.

6. Goodman, Jordan. *Tobacco in History and Culture: An Encyclopedia* (Detroit: Thomson Gale, 2005).
7. Heckewelder, *History, Manners and Customs of the Indian Nations who Once Inhabited Pennsylvania*, p. 149 ff.
8. "They smoke with excessive eagerness ... men, women, girls and boys, all find their keenest pleasure in this way." - Dièreville describing the Mi'kmaq, *circa* 1699 in *Port Royal*.
9. Jack Jacob Gottsegen, *Tobacco: A Study of Its Consumption in the United States*, 1940, p. 107.
10. Ganapathi TR; et al. (2004). "Tobacco (Nicotiana tabacum L.) – A model system for tissue culture interventions and genetic engineering" (PDF). *Indian Journal of Biotechnology*. 3: 171–184.
11. Fraley RT; et al. (1983). "Expression of bacterial genes in plant cells". *Proc. Natl. Acad. Sci. U.S.A.* 80 (15): 4803–4807. Bibcode:1983PNAS...80.4803F. doi:10.1073/pnas.80.15.4803. PMC 384133. PMID 6308651.
12. "Science of Transgenic Cotton". Cottoncrc.org.au. Archived from the original on March 21, 2012. Retrieved October 3, 2013.
13. Gonzalez FJ, Gelboin HV (November 1992). "Human cytochromes P450: evolution and cDNA-directed expression". *Environmental Health Perspectives*. 98: 81–5. doi:10.1289/ehp.929881. PMC 1519618. PMID 1486867.
14. "Cytochrome P450". *InterPro*.
15. Danielson PB (December 2002). "The cytochrome P450 superfamily: biochemistry, evolution and drug metabolism in humans". *Current Drug Metabolism*. **3** (6): 561–97. doi:10.2174/1389200023337054. PMID 12369887.
16. Berka K, Hendrychová T, Anzenbacher P, Otyepka M (October 2011). "Membrane position of ibuprofen agrees with suggested access path entrance to cytochrome P450 2C9 active site". *The Journal of Physical Chemistry A*. **115** (41): 11248–55. Bibcode:2011JPCA..11511248B. doi:10.1021/jp204488j. PMC 3257864. PMID 21744854.
17. Guengerich FP (January 2008). "Cytochrome p450 and chemical toxicology". *Chemical Research in Toxicology*. **21** (1): 70–83. doi:10.1021/tx700079z. PMID 18052394. S2CID 17548932. (Metabolism in this context is the chemical modification or degradation of drugs.)
18. McLean KJ, Clift D, Lewis DG, Sabri M, Balding PR, Sutcliffe MJ, Leys D, Munro AW (May 2006). "The preponderance of P450s in the Mycobacterium tuberculosis genome". *Trends in Microbiology*. **14** (5): 220–8. doi:10.1016/j.tim.2006.03.002. PMID 16581251.
19. Ikeda H, Ishikawa J, Hanamoto A, Shinose M, Kikuchi H, Shiba T, Sakaki Y, Hattori M, Omura S (May 2003). "Complete genome sequence and comparative analysis of the industrial microorganism Streptomyces avermitilis". *Nature Biotechnology*. **21** (5): 526–31. doi:10.1038/nbt820. PMID 12692562.
20. Smith, J. N., Mehinagic, D., Nag, S., Crowell, S. R., & Corley, R. A. (2017). In vitro metabolism of benzo[a]pyrene-7,8-dihydrodiol and dibenzo[def,p]chrysene-11,12 diol in rodent and human hepatic microsomes. *Toxicology letters*, *269*, 23–32. https://doi.org/10.1016/j.toxlet.2017.01.008
21. Aggunna, M., Grandhi, A.V.K.S. and Yedidi, R.S. (2022). TCABSE-J, Vol. 1, Issue 3. Epub: Apr 2nd , 2022.

Acknowledgements: The authors thank T*yi*DE-Toronto, Canada for helping to write this manuscript. KM thanks Ms. Madhuri Vissapragada and Mr. Manikanta Sodasani for their help and support in the laboratory.

Funding: The authors thank TCABS-E, Rajahmundry, India and T*yi*DE-Toronto, Canada for financial support.

Conflict of interest: This research article is an ongoing project currently at TCABS-E, Rajahmundry, India.

TCABSE-J Research Article
ISSN: 2583- 2557, *Volume 1, Issue 4, pp9-17. 2022.*

TCABSE-J
Interdisciplinary Sciences Journal

Novel biophysical strategy for the delivery of therapeutic microRNA molecules for Cancer and infectious diseases treatment.

[1, 2]Manisha Lanka, [1]Manikanta Sodasani and [1, 3]Ravikiran S. Yedidi*

[1]The Center for Advanced-Applied Biological Sciences & Entrepreneurship (TCABS-E), Visakhapatnam 530016, AP; [2]Department of Biochemistry, [3]Department of Zoology, Andhra University, Visakhapatnam 530003, AP. (*Correspondence to RSY: tcabse.india@gmail.com)

Cancer is the most common disease worldwide and accounts for the highest number of deaths. The number of therapies available in the medical field is not yet sufficient to cure cancer. The numerous existing diagnostic methods are not cost-effective and insufficient to detect cancer in its early stages. With increasing access to tobacco and the industrialization of nations, lung cancer has become the most common cancer of the 20th century, and deaths from lung cancer have steadily increased since the early 20th century. MicroRNAs are used as therapeutics in various tumors, infections and metabolic diseases. They have been used more widely over the past decade as they can inhibit the translation process. MicroRNAs can also be used as biomarkers and help us identify early stage cancer. Current microRNA delivery systems are not 100% effective and have side effects such as inflammation etc. In this experiment we check the feasibility of microRNAs delivery using novel methods such as liquid-liquid phase separation. The genes responsible for the mutations in lung cancer are identified and the associated microRNAs target sites are identified using computational databases and software. In the case of RNA and proteins, the phase separation of the liquid droplets is observed and suggests a positive outcome.

Keywords: miRNAs, Liquid-Liquid Phase separation, Protein Droplets, Lung cancer, drug delivery.

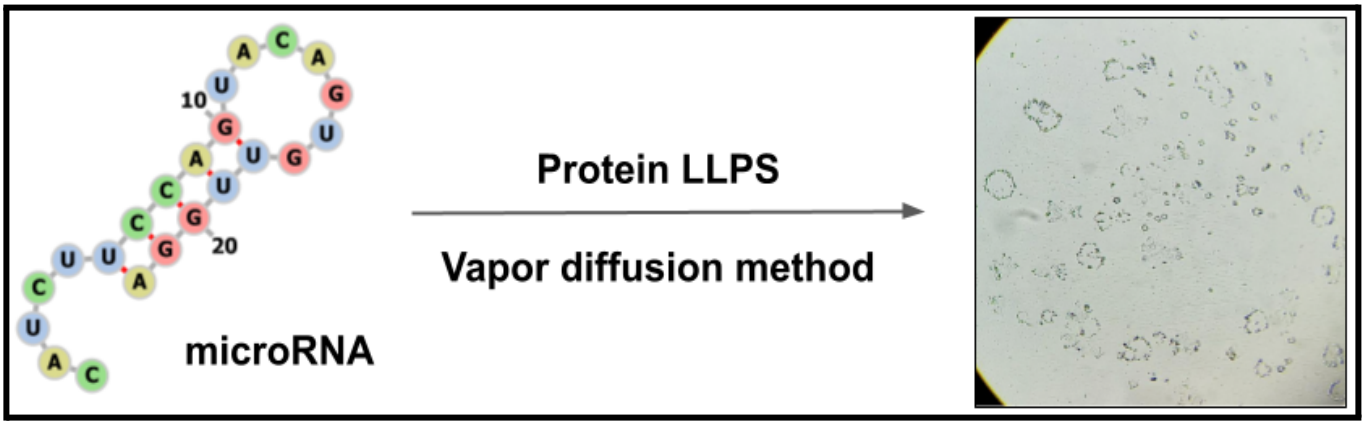

Figure 1. Overview of protein-RNA liquid-liquid phase separation using vapor diffusion method.

Citation: Lanka, M., Sodasani, M. and Yedidi, R. S. (2022). Novel biophysical strategy for the delivery of therapeutic microRNA molecules for Cancer and infectious diseases treatment. *TCABSE-J*, Vol. 1, Issue 4:9-17. Epub: Oct5th, 2022.

CANCER: Cancer is a set of diseases that have afflicted living beings for more than 200 million years. Cancer is caused by human cells growing out of control and spreading to other parts of the body [1]. The causes of cancer can be varied, such as smoking, obesity, genetic changes, radiation, diet, physical activity, etc. The causes were also linked to occupations. People who worked in asbestos mines were more prone to lung cancer and radiologists were more prone to skin cancer because of the harmful X-rays [2]. The types of genes implicated in the cause of cancer are oncogenes, tumor suppressor genes, and DNA repair genes [3]. The oncogenes are the cancer-causing genes that turn a healthy cell into a cancerous cell. It is known that these changes are inherited [4]. The tumor suppressor genes are generally protective genes, but when they mutate, they grow uncontrollably and form cancer [4]. Errors in DNA repair genes can cause mutations and eventually lead to cancer [4]. There are no particular signs and symptoms in the early stages of cancer, but they appear as the mass grows [5]. Cancer originates in one place, enters the bloodstream, and spreads to other parts of the body. This is known as cancer metastasis [6]. Metastases are common in the late stages of cancer [5][6]. Some cancers spread to specific parts of the body - Breast cancer tends to spread to the bones, liver, lungs, chest wall, and brain, lung cancer tends to spread to the brain, bones, liver, and adrenal glands, prostate cancer tends to spread to the bones, colon and rectal cancers tend to spread to the liver and lungs [7]. The types of cancers include carcinoma, sarcoma, leukemia, and lymphoma based on where they begin [4][5]. Estimated epidemiological trends from 2016 to 2060 predicted that liver cancer, gastric cancer, colorectal cancer, breast cancer, and lung cancer would be the most common, with lung cancer having the highest incidence worldwide [8]. These numbers could just keep rising in the absence of proper diagnostic methods and treatments. Prevention is the way to reduce the risk of cancer.

LUNG CANCER: Lung cancer is the most commonly diagnosed type of cancer worldwide. Lung cancer has the highest mortality rate in both men and women [9]. A mass grows in the lungs and grows out of control, leading to tumors. Smoking is the main cause of lung cancer although it has been found in some non-smokers due to many reasons such as environmental pollution, secondhand smoke, occupational exposure, etc [10]. The chance of getting lung cancer is very low after quitting smoking [9]. The other factors include genetics, age, gender, etc. which can cause lung cancer. Genetic mutations could be another major cause of lung cancer. The types of lung cancer are non-small cell lung cancer (NSCLC) and small cell lung cancer (SCLC) [11]. NSCLC is a type of epithelial lung cancer that accounts for approximately 85% of all lung cancers [12]. The most common genetic mutations in people with NSCLC include KRAS, EGFR, ALK, MET, FGFR1, PIK3CA, BRAF, ROS1, etc. NSCLC is less aggressive than SCLC but is difficult to diagnose and has more deaths worldwide. The most common subtypes of NSCLC are adenocarcinoma (40%), squamous cell carcinoma (25%), and large cell carcinoma (10%) [12][13]. Adenocarcinoma is the most common type of cancer in non-smokers [14]. Squamous cell carcinomas begin in the squamous cells and migrate to the central parts of the lungs. The most common cause of squamous cell carcinoma is tobacco smoke [15]. Large cell carcinoma can grow in any part of the lung and tends to grow and spread rapidly [16]. Symptoms of NSCLC include cough, pleural effusion, shortness of breath, weight loss, malaise, etc. Small cell lung cancer (SCLC) accounts for about 12% of lung cancer cases, is more aggressive, and spreads easily compared to NSCLC [13]. SCLC starts in the bronchi and spreads to other parts of the lung quickly [17]. It is easy to diagnose as it spreads rapidly. SCLC is common in people who smoke. The treatment for lung cancer includes chemotherapy, immunotherapy, radiation, surgery, etc [12][17].

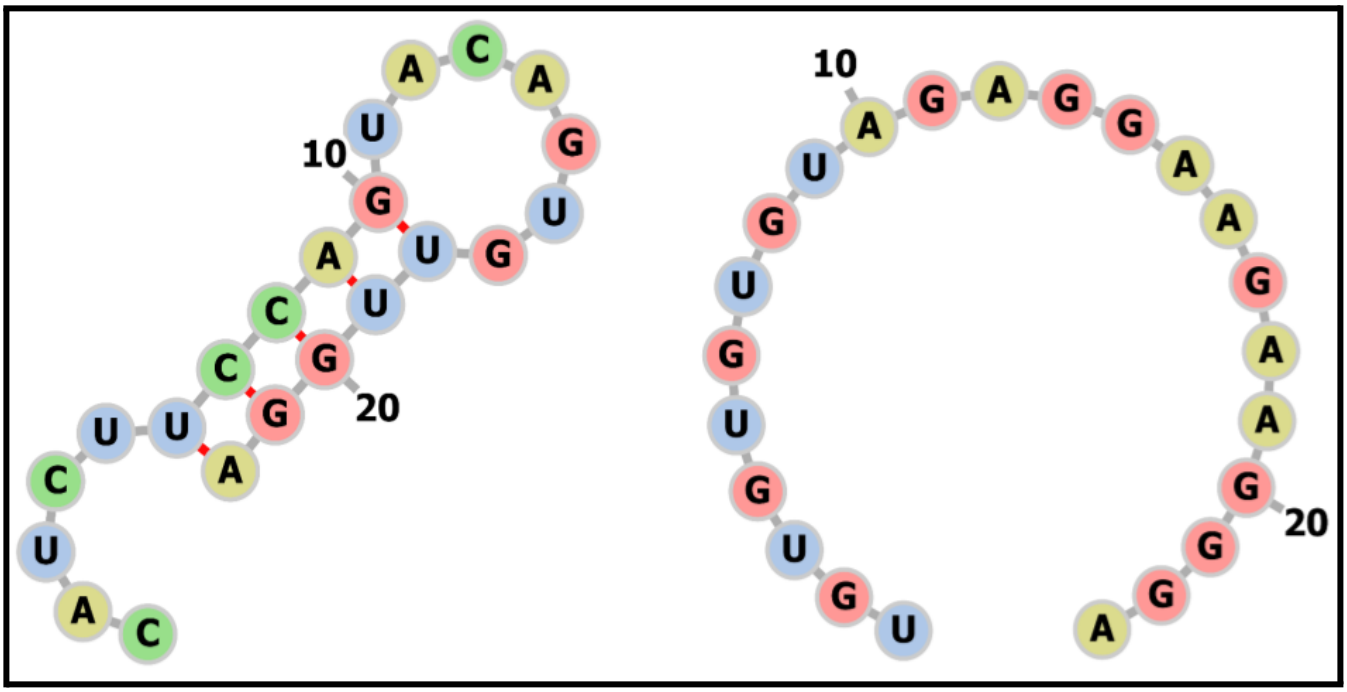

Figure 2. miRNAs with and without self-complementarity.

Lung cancer was a rare disease at the beginning of the 20th century, but due to reasons such as an increase in the number of smokers, environmental pollution, occupational exposure, etc., it has become a plague at the end of the 20th century [18]. About 10% to 20% of lung cancer cases are never-smokers in Asian women [19]. Despite the new technologies and advances in medicine and research, the survival rate from lung cancer does not exceed 5 years, even with the help of numerous therapies, because by the time the cancer is diagnosed, cancer has already progressed to other parts of the body [20]. The mortality rate from lung cancer is three times higher in men than from prostate cancer and twice as high in women than from breast cancer [21]. According to the International Agency for Research on Cancer (IARC), the number of lung cancer cases could increase by 45% in 2040 [22]. Lung cancer deaths are higher than colorectal, breast, prostate, and pancreatic cancers combined [23]. The survival rate varied for localized cancer (stage I-II), regional cancer (stage III), and metastatic cancer (stage IV), with localized cancer having a better survival rate compared to regional and metastatic cancer [24]. The survival rate depends on factors such as gender, age, socio economic impact, type of cancer (either NSCLC or SCLC), stage of cancer, etc [25][26]. About 40% of people survive 1 year after diagnosis, 15% survive 5 years after diagnosis and 10% survive 10 years after diagnosis [26]. Underprivileged nations are at higher risk of cigarette smoking and poor lung cancer survival rates.

NON-CODING RNAs: RNA generally undergoes translation to give corresponding proteins. But certain RNAs do not participate in the translation process and do not form a protein. These RNAs are referred to as non-coding RNAs (ncRNAs) [27]. There are two types of non-coding RNAs: housekeeping ncRNAs and regulatory ncRNAs. Housekeeping ncRNAs include ribosomal RNA (rRNA), and transfer RNA (tRNA), which normally serve essential functions of the cell such as translation, small nuclear RNA (snRNA), which is involved in splicing, and small nucleolar RNA (snoRNAs), which are involved in the modification of RNA [28][29]. The regulatory

ncRNAs include short ncRNAs and long ncRNAs. The short ncRNAs are micro-RNA (miRNA), small interfering RNA (siRNA), and piwi-interacting RNA (piRNA), which are <200 nucleotides in length. The long ncRNAs are competitive endogenous RNA (ceRNA) and enhancer-derived RNA (eRNA) that are >200 nucleotides in length [30]. The regulatory ncRNAs are from 1% of the total genome [31]. The regulatory ncRNAs play an important role in regulating the various processes of the cell and other networks [32]. The short ncRNAs - siRNA and miRNA are similar in length and participate in the RNA Interference pathway (RNAi) [33]. The RNAi pathway, also called post-transcriptional gene silencing, is the process of sequence-specific gene suppression [34]. In the RNAi pathway, the short RNA binds to the DNA and inhibits the gene expression [35].

MICRO-RNAs: MicroRNAs (miRNA/miR) are short, non-coding RNAs approximately 22-25 nucleotides in length. The miRNAs are single-stranded RNA molecules that help in the RNAi pathway by binding to the mRNA molecule [36]. The miRNAs were first discovered in the early 1990s in the larval form of *C.elegans*. Let-7 was the first miRNA to be discovered, and let-7 was found to play an important role in the development of the later larval stage to an adult [37]. miRNA gene or intron was first transcripted into pri-miRNA with the help of RNA Pol II/III in the nucleus. The pri-miRNA is cleaved with Drosha and DGCR8 to form a pre-miRNA. The pre-miRNA is now transported to the cytoplasm with the help of a transporter molecule called Exportin-5 in combination with Ran-GTP. The pre-miRNA is cleaved with Dicer to form a miR duplex. Argonaute proteins act on the duplex and break down one of the strands and help form the RNA-Induced Silencing Complex (RISC) and they process to form a mature microRNA. The mature microRNA can now function in various cellular processes such as translational repression, mRNA deadenylation, etc [36][37][38][39]. MicroRNA functions include a) post-initiation mechanisms - miRNAs block translation elongation, b) co-translational protein degradation - polypeptide chain is degraded, c) miR-mediated mRNA decay - deadenylation and decapping, d) inhibition mechanisms - inhibition of ribosomal subunit joining, competition for cap structure and inhibition of mRNA circularization by deadenylation [40].

There are two types of cancer-associated microRNAs - OncomiRs and tumor-suppressing miRs. The dysregulation of certain miRs leads to the formation of OncomiRs [41]. The tumor suppressor miRs generally help down-regulate the oncogenes. But in some cases, when the number of tumor-suppressing miRs is reduced, oncogenes leading to cancer are rapidly produced [42]. Tumor suppressor miRNAs are used in gene therapies to inhibit cancer progression. miRNA masking, small molecule inhibitors, miRNA sponges, etc are used to downregulate OncomiRs [42]. The RNAi pathway has gained a lot of favor because of its significance as an experimental tool [43]. Various therapeutics are currently available for cancer, such as small molecules, antibodies, etc. Limitations include that the therapy only works when the tumor has a specific target and cannot lead to long-term efficacy [44]. MicroRNAs can act on multiple targets simultaneously and can efficiently inhibit the gene expression of the cancer-causing genes [45]. MicroRNAs also act as biomarkers for various diseases as they circulate in the bloodstream [46]. The imaging and invasive techniques currently used to diagnose cancer can be very costly and uncomfortable for patients [47]. MiRNAs can be used for prediction and prognosis purposes [46]. Only the blood sample is required to identify the miRNAs [47].

Various delivery systems are in practice to efficiently deliver the miRNAs to the tumor microenvironment. The vectors are viral vectors and non-viral vectors [48]. The viral vectors are the genetically engineered viruses that can carry oligonucleotides. The types of viral vectors include

retroviral vectors, adenoviral vectors, lentivirus vectors, bacteriophage associated vectors [49]. The viral vectors are useful because of their low immunogenicity and stable gene expression, but also have disadvantages such as low packaging capacity, viruses that do not replicate in the host cell leading to infections, and high carcinogenic potential due to insertional mutagenesis [49][50]. Non-viral vectors include inorganic materials, lipid-based nanocarriers, polymeric vectors, etc. [48]. The inorganic particles like gold and silicon are used in nanotechnologies to deliver miRNAs. The lipid-based nanocarriers include cationic NLCs, neutral NLCs, and target-modified NLCs. The disadvantages include lack of targeting efficiency, low packing efficiency, etc. [51].

LIQUID-LIQUID PHASE SEPARATION (LLPS): Phase separation is a process in which an immiscible liquid is separated from the mixture into two distinct components. LLPS is a reversible physicochemical phenomenon that consists in the mixing of two distinct liquid phases with different solute concentrations [52]. It is a biological procedure in the cells where the condensates appear like oil droplets in water under various interacting forces[53]. Macromolecules condense with the liquid droplets, forming condensates that contribute to many biological processes and regulatory mechanisms [52][54]. The molecules condense into a dense phase and the dense phase coexists with the aqueous phase. LLPS is a relatively new biophysical method first described by Brangwynne *et. al* as a phase-separated condensate of RNA and proteins [55]. Eukaryotic cells have membrane-bound organe -lles (Endoplasmic Reticulum) and membrane -less organelles (Stress granules) [56]. LLPS is the underlying mechanism for the formation of membrane-less organelles and their functions [56][57]. The driving forces of LLPS include assembly, sequestration, reaction crucible, packaging transports, protein-protein and protein-RNA interactions, weak interactions between intrinsically disordered regions [56]. Databases like (LLPSDB, PhaSePro, PhaSepDB, DrLLPS, RNAgranule -DB, and HUMAN CELLMAP) are developed to identify the membrane-less organelles based on LLPS [58]. Interactions between droplets and enzymatic solutes will achieve functions such as protocell formation, applications such as drug delivery vehicles, and so on [59]. In this study, the total cellular RNA was mixed with proteins to set up the hanging drop vapor diffusion droplets in order to evaluate the formation of LLPS. This will serve as a prototype for future studies.

Materials & Methods:

NCBI search: Five genes were identified as the most mutating genes in lung cancer. The five genes include KRAS, EGFR, FGFR1, ALK, MET. KRAS is the highly mutated gene and MET is the gene that mutates about 1% in the cases of lung cancer. EGFR has the most number of mutations after KRAS. In this study, we focus on EGFR which accounts for 10%-25% of the cases. The gene EGFR was searched in the gene database of NCBI, and 9 transcript variants were found. Using mirdb.org, microRNAs related to EGFR were listed based on their target scores and target ranks. 118 microRNAs were found to have more than 60 target scores. Of the 118 microRNAs, they were further filtered out based on their self-complementarities. The microRNAs with no self-complementarities are preferred.

Computing the RNA secondary structure: The secondary structures of the 118 microRNAs were predicted using the RNAfold web server. The sequences of the microRNAs were pasted into the webserver and the secondary structures were analyzed. The microRNAs with no self-complementarities were preferred as they can bind perfectly to the gene sequence without binding to themselves. Fourteen out of 118 microRNAs were found to be without any self-complementarities whicher were chosen for further study to avoid any self-complementarity bias.

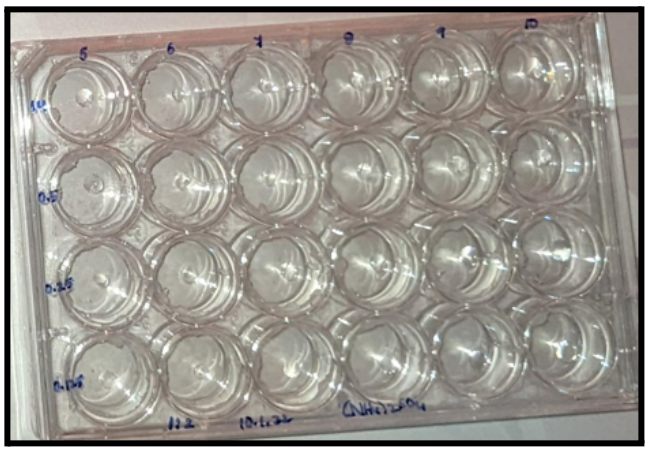

Figure 3. A 24-well plate showing hanging drops.

The microRNAs of the EGFR gene till the 92 target score were taken and aligned using ClustalO, to check if all the microRNAs have the same 3'-UTR sequence. The microRNAs are aligned in a perfect way which indicates that all the microRNAs have the same 3'-UTR sequence. The 3'-UTR sequences of the microRNAs are now aligned with the EGFR transcript variants with the help of the Global Align of BLAST database from NCBI. The Global Align results helped in the identification of the CDS and the 3'-UTR sequence.

Hanging drop vapor diffusion plates: First, pilot studies were performed with protein and buffer to verify phase separation. To carry out the liquid-liquid phase separation experiments, two buffers with different pH values and different molarities were prepared. The two buffers are sodium chloride (NaCl) and ammonium sulfate ($(NH_4)_2SO_4$) with different molarities of 1 M, 0.5 M, 0.25 M, and 0.125 M are prepared. The different molar buffers are now adjusted to different pH values with 1N HCl or 1N NaCl as acid or base. The different pH values are 5,6,7,8,9,10. The various tubes of the pH are labeled accordingly. The 24-well tissue culture plates were taken to fix the protein droplets. The 24-well plate is now filled with 1 ml of the buffer of different molarities and pH values. The four rows of the plate have four different molarities and the six columns each have different pH values of the buffer. The pilot experiments are carried out under four conditions. Protein and buffer are mixed in ratios of 1:2 and 2:2 with NaCl and (NH4)2SO4. Four plates were fixed with the ratios 1:2 protein:NaCl, 2:2 protein:NaCl, 1:2 protein:$(NH_4)_2SO_4$ and 2:2 protein:$(NH_4)_2SO_4$. A total of 2μl drops were placed on the coverslip and mixed with the micropipette. The coverslip was carefully placed on the wells of the tissue culture plate. The plates were left undisturbed for 2 weeks to allow the droplets to condense. The plates are later viewed under the microscope to observe phase separation. The same experiments are now conducted with protein, buffer, and whole-cell RNA molecules. These experiments are carried out under two conditions. Protein, RNA, and buffer are mixed in ratios of 0.5:0.5:1 with NaCl and $(NH_4)_2SO_4$. A total of 2μl drop was placed on the coverslip and mixed with the micropipette. The coverslip was carefully placed on the wells of the tissue culture plate. The plates were left undisturbed for 2 weeks to allow the droplets to condense. The plates are later viewed under the microscope to observe phase separation.

Results and Discussion:

LLPS were obtained in multiple conditions: For the experiments conducted with protein, RNA and buffer, phase separation is observed in the following five conditions of which three wee prominently visible as shown in Figure 4:

(i.) [0.5:0.5:1 protein:RNA:NaCl] ; buffer concentration - 0.5M, pH - 10.
(ii.) [0.5:0.5:1 protein:RNA:NaCl] ; buffer concentration - 0.25M, pH - 6.
(iii.) [0.5:0.5:1 protein:RNA:NaCl] ; buffer concentration - 0.25M, pH - 8.
(iv.) [0.5:0.5:1 protein:RNA:$(NH_4)_2SO_4$]; buffer concentration - 0.5M, pH - 10.
(v.) [0.5:0.5:1 protein:RNA:$(NH_4)_2SO_4$]; buffer concentration - 0.125M, pH - 8.

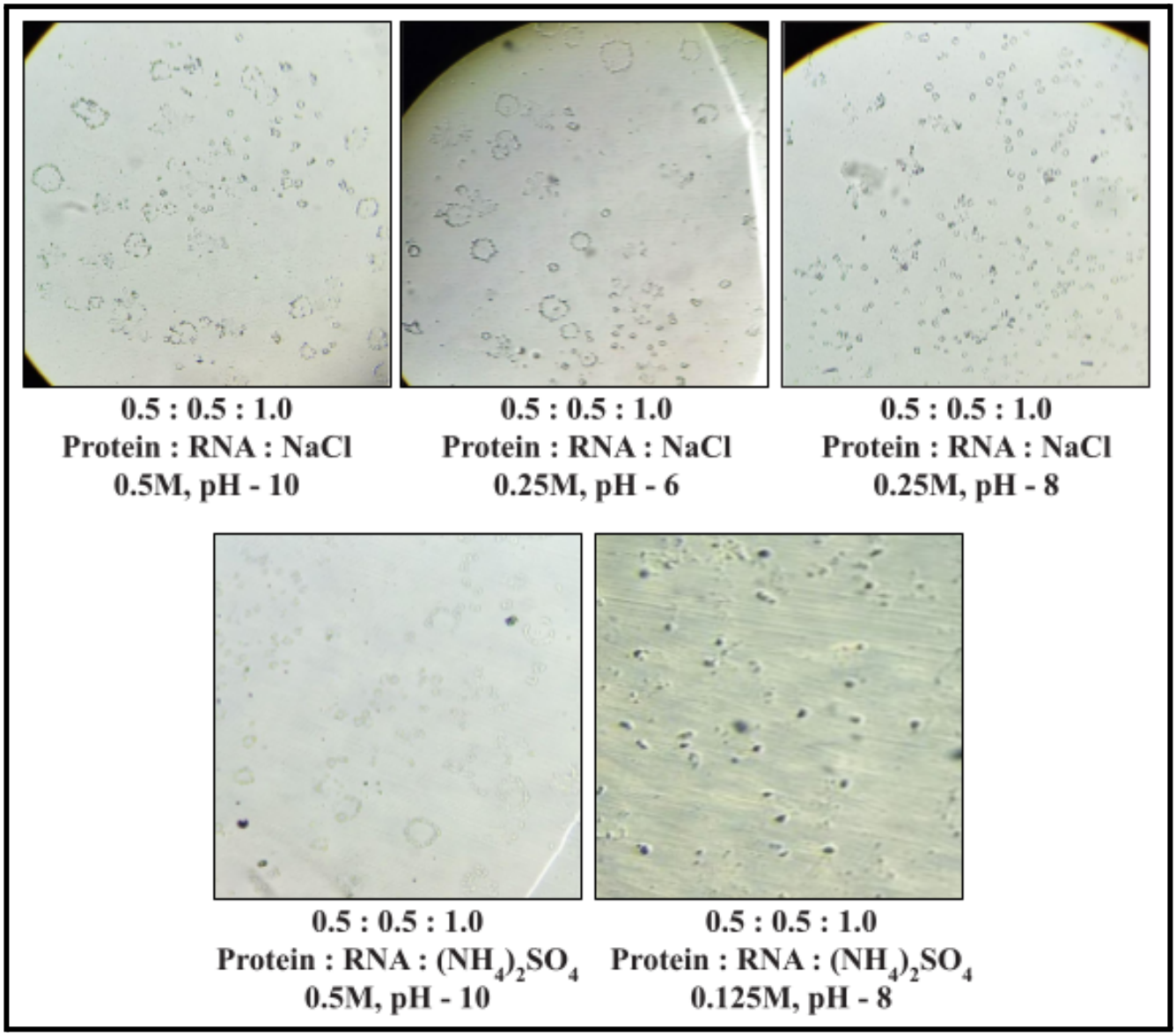

Figure 4. Hit conditions that showed LLPS of protein-RNA.

The present study clearly demonstrates that it is indeed possible to obtain liquid-liquid phase separations (LLPS) using a mixture of protein and microRNA. The hit conditions will be further expanded to fine tune the exact conditions of the LLPS. Based on the results in this study we conclude that it is possible to obtain LLPS using protein-RNA mixtures and in future, these hit conditions will be used as novel drug delivery systems. We will check the phase separation with different proteins to find out which protein is the best. We will examine the different sizes and concentrations of microRNAs to test the concentration at which phase separation can be performed with RNAs. The current study has tested and proved that it is indeed possible to obtain LLPS droplets not only with proteins but also with a mixture of protein-RNA. These results suggest that the protein-RNA mixed LLPS droplets can be evaluated further for the feasibility of microRNA delivery as a therapeutic approach.

References

1. Hausman, Daniel M. (2019). *What Is Cancer?. Perspectives in Biology and Medicine, 62(4), 778–784.* doi:10.1353/pbm.2019.0046
2. Blackadar, Clarke Brian (2016). *Historical review of the causes of cancer. World Journal of Clinical Oncology, 7(1), 54–.* doi:10.5306/wjco.v7.i1.54
3. https://www.cancer.gov/about-cancer/understanding/what-is-cancer
4. https://www.cancer.net/navigating-cancer-care/cancer-basics/genetics/genetics-cancer#:~:text=The%20most%20commonly%20mutated%20gene,many%20different%20types%20of%20cancer
5. Wikipedia contributors. "Cancer." *Wikipedia, The Free Encyclopedia*. Wikipedia, The Free Encyclopedia, 10 Apr. 2022. Web. 10 Apr. 2022.
6. https://my.clevelandclinic.org/health/diseases/22213-metastasis-metastatic-cancer
7. https://www.cancer.net/navigating-cancer-care/cancer-basics/what-metastasis
8. Mattiuzzi, Camilla; Lippi, Giuseppe (2019). *Current Cancer Epidemiology. Journal of Epidemiology and Global Health, 9(4), 217–.* doi:10.2991/jegh.k.191008.001
9. Nasim, Faria; Sabath, Bruce F.; Eapen, George A. (2019). *Lung Cancer. Medical Clinics of North America, 103(3), 463–473.* doi:10.1016/j.mcna.2018.12.006
10. Bade, Brett C.; Dela Cruz, Charles S. (2020). *Lung Cancer 2020. Clinics in Chest Medicine, 41(1), 1–24.* doi:10.1016/j.ccm.2019.10.001
11. Wikipedia contributors. "Lung cancer." *Wikipedia, The Free Encyclopedia*. Wikipedia, The Free Encyclopedia, 21 Mar. 2022. Web. 11 Apr. 2022.
12. Wikipedia contributors. "Non-small-cell lung carcinoma." *Wikipedia, The Free Encyclopedia*. Wikipedia, The Free Encyclopedia, 7 Mar. 2022. Web. 11 Apr. 2022.
13. https://www.cancer.org/cancer/lung-cancer/about/what-is.html
14. Myers DJ, Wallen JM. Lung Adenocarcinoma. [Updated 2021 Sep 10]. In: StatPearls [Internet]. Treasure Island (FL): StatPearls Publishing; 2022 Jan-. Available from: https://www.ncbi.nlm.nih.gov/books/NBK519578/
15. Sabbula BR, Anjum F. Squamous Cell Lung Cancer. [Updated 2021 Dec 8]. In: StatPearls [Internet]. Treasure Island (FL): StatPearls Publishing; 2022 Jan-. Available from: https://www.ncbi.nlm.nih.gov/books/NBK564510/
16. Wikipedia contributors. "Large-cell lung carcinoma." *Wikipedia, The Free Encyclopedia*. Wikipedia, The Free Encyclopedia, 12 Nov. 2021. Web. 11 Apr. 2022.
17. Wikipedia contributors. "Small-cell carcinoma." *Wikipedia, The Free Encyclopedia*. Wikipedia, The Free Encyclopedia, 14 Feb. 2022. Web. 14 Apr. 2022.
18. Alberg, Anthony J.; Samet, Jonathan M. (2003). *Epidemiology of Lung Cancer*. Chest, 123(1), 21S–49S.* doi:10.1378/chest.123.1_suppl.21S
19. Barta, Julie A et al. "Global Epidemiology of Lung Cancer." *Annals of global health* vol. 85,1 8. 22 Jan. 2019, doi:10.5334/aogh.2419
20. Youlden, Danny R.; Cramb, Susanna M.; Baade, Peter D. (2008). *The International Epidemiology of Lung Cancer: Geographical Distribution and Secular Trends. Journal of Thoracic Oncology, 3(8), 819–831.* doi:10.1097/JTO.0b013e31818020eb
21. E. Goodarzi, M. Sohrabivafa , H.A. Adineh , L. Moayed , Z. Khazaei. *Geographical distribution global incidence and mortality of lung cancer and its relationship with the human development index (HDI); An Ecology study in 2018. World Cancer Research Journal.* WCRJ 2019; 6: e1354
22. Kastner, Julia; Hossain, Rydhwana; Whilte, Charles (2019). *Epidemiology of Lung Cancer. Seminars in Roentgenology, (), S0037198X1930077X–.* doi:10.1053/j.ro.2019.10.003
23. Dela Cruz, Charles S.; Tanoue, Lynn T.; Matthay, Richard A. (2011). *Lung Cancer: Epidemiology, Etiology, and Prevention. Clinics in Chest Medicine, 32(4), 605–644.* doi:10.1016/j.ccm.2011.09.001
24. Thandra KC, Barsouk A, Saginala K, Aluru JS, Barsouk A. Epidemiology of lung cancer. Contemp Oncol (Pozn). 2021;25(1):45-52. doi: 10.5114/wo.2021.103829. Epub 2021 Feb 23. PMID: 33911981; PMCID: PMC8063897.
25. Rafiemanesh, Hosein; Mehtarpour, Mojtaba; Khani, Farah; Hesami, Sayed Mohammadali; Shamlou, Reza; Towhidi, Farhad; Salehiniya, Hamid; Makhsosi, Behnam Reza; Moini, Ali (2016). *Epidemiology, incidence and mortality of lung cancer and their relationship with the development index in the world. Journal of Thoracic Disease, 8(6), 1094–1102.* doi:10.21037/jtd.2016.03.91
26. https://www.webmd.com/lung-cancer/guide/lung-cancer-survival-rates
27. Wikipedia contributors. "Non-coding RNA." *Wikipedia, The Free Encyclopedia*. Wikipedia, The Free Encyclopedia, 28 Feb. 2022. Web. 9 Apr. 2022.
28. John S. Mattick, Igor V. Makunin, Non-coding RNA, *Human Molecular Genetics*, Volume 15, Issue suppl_1, 15 April 2006, Pages R17–R29, https://doi.org/10.1093/hmg/ddl046
29. Wei, Jian-Wei; Huang, Kai; Yang, Chao; Kang, Chun-Sheng (2016). *Non-coding RNAs as regulators in epigenetics (Review). Oncology Reports.* doi:10.3892/or.2016.5236
30. Statello, L., Guo, CJ., Chen, LL. *et al.* Gene regulation by long non-coding RNAs and its biological functions. *Nat Rev Mol Cell Biol* 22, 96–118 (2021). https://doi.org/10.1038/s41580-020-00315-9
31. Palazzo, Alexander F.; Lee, Eliza S. (2015). *Non-coding RNA: what is functional and what is junk?. Frontiers in Genetics, 6.* doi:10.3389/fgene.2015.00002
32. Bhogireddy, S., Mangrauthia, S.K., Kumar, R. *et al.* Regulatory non-coding RNAs: a new frontier in regulation of plant biology. *Funct Integr Genomics* 21, 313–330 (2021). https://doi.org/10.1007/s10142-021-00787-8
33. Wikipedia contributors. "Small interfering RNA." *Wikipedia, The Free Encyclopedia*. Wikipedia, The Free Encyclopedia, 28 Mar. 2022. Web. 10 Apr. 2022.
34. Wikipedia contributors. "RNA interference." *Wikipedia, The Free Encyclopedia*. Wikipedia, The Free Encyclopedia, 2 Apr. 2022. Web. 10 Apr. 2022.
35. Jens Kurreck (2009). *RNA Interference: From Basic Research to Therapeutic Applications. , 48(8), 1378–1398.* doi:10.1002/anie.200802092

36. Wikipedia contributors. "MicroRNA." *Wikipedia, The Free Encyclopedia*. Wikipedia, The Free Encyclopedia, 2 Apr. 2022. Web. 10 Apr. 2022.
37. Bhaskaran, M, and M Mohan. "MicroRNAs: history, biogenesis, and their evolving role in animal development and disease." *Veterinary pathology* vol. 51,4 (2014): 759-74. doi:10.1177/0300985813502820
38. O'Brien, Jacob; Hayder, Heyam; Zayed, Yara; Peng, Chun (2018). *Overview of MicroRNA Biogenesis, Mechanisms of Actions, and Circulation. Frontiers in Endocrinology, 9(), 402–*. doi:10.3389/fendo.2018.00402
39. Zeng, Y (2006). *Principles of micro-RNA production and maturation. , 25(46), 6156–6162.* doi:10.1038/sj.onc.1209908
40. Ana Eulalio; Eric Huntzinger; Elisa Izaurralde (2008). *Getting to the Root of miRNA-Mediated Gene Silencing. , 132(1), 0–14.* doi:10.1016/j.cell.2007.12.024
41. Wikipedia contributors. "Oncomir." *Wikipedia, The Free Encyclopedia*. Wikipedia, The Free Encyclopedia, 30 Dec. 2021. Web. 10 Apr. 2022.
42. Gambari, Roberto et al. "Targeting oncomiRNAs and mimicking tumor suppressor miRNAs: New trends in the development of miRNA therapeutic strategies in oncology (Review)." *International journal of oncology* vol. 49,1 (2016): 5-32. doi:10.3892/ijo.2016.3503
43. Scott M. Hammond (2006). *RNAi, microRNAs, and human disease. , 58(1 Supplement), 63–68.* doi:10.1007/s00280-006-0318-2
44. https://interna-technologies.com/our-science/mirna-therapeutics/
45. Van Rooij, E.; Kauppinen, S. (2014). *Development of microRNA therapeutics is coming of age. EMBO Molecular Medicine, 6(7), 851–864.* doi:10.15252/emmm.201100899
46. Felekkis, Kyriacos; Papaneophytou, Christos (2020). *Challenges in Using Circulating Micro-RNAs as Biomarkers for Cardiovascular Diseases. International Journal of Molecular Sciences, 21(2), 561–*. doi:10.3390/ijms21020561
47. Sundarbose, Kamini & Kartha, Reena & Subramanian, Subbaya. (2013). MicroRNAs as Biomarkers in Cancer. Diagnostics. 3. 84-104. 10.3390/diagnostics3010084.
48. Fu, Y., Chen, J. & Huang, Z. Recent progress in microRNA-based delivery systems for the treatment of human disease. *ExRNA* 1, 24 (2019). https://doi.org/10.1186/s41544-019-0024-y
49. Dasgupta I, Chatterjee A. Recent Advances in miRNA Delivery Systems. *Methods and Protocols*. 2021; 4(1):10. https://doi.org/10.3390/mps4010010
50. Kolliopoulou, Anna; Taning, Clauvis N. T.; Smagghe, Guy; Swevers, Luc (2017). *Viral Delivery of dsRNA for Control of Insect Agricultural Pests and Vectors of Human Disease: Prospects and Challenges. Frontiers in Physiology, 8(), 399–*. doi:10.3389/fphys.2017.00399
51. Wang, H., Liu, S., Jia, L. *et al.* Nanostructured lipid carriers for MicroRNA delivery in tumor gene therapy. *Cancer Cell Int* 18, 101 (2018). https://doi.org/10.1186/s12935-018-0596-x
52. https://encyclopedia.pub/entry/7187#:~:text=Liquid%E2%80%93liquid%20phase%20separation%20(LLPS,phases%2C%20with%20different%20solute%20concentrations.
53. Qi Guo;Xiangmin Shi;Xiangting Wang; (2021). *RNA and liquid-liquid phase separation . Non-coding RNA Research.* doi:10.1016/j.ncrna.2021.04.003
54. Shin, Yongdae; Brangwynne, Clifford P. (2017). *Liquid phase condensation in cell physiology and disease. Science, 357(6357), eaaf4382–*. doi:10.1126/science.aaf4382
55. Kamimura, Yugo R., and Motomu Kanai. "Chemical Insights into Liquid-Liquid Phase Separation in Molecular Biology." *Bulletin of the Chemical Society of Japan* 1 Mar. 2021: 1045–1058. *Bulletin of the Chemical Society of Japan*. Web.
56. Wang, B., Zhang, L., Dai, T. *et al.* Liquid–liquid phase separation in human health and diseases. *Sig Transduct Target Ther* 6, 290 (2021). https://doi.org/10.1038/s41392-021-00678-1
57. Alberti, Simon et al. "Considerations and Challenges in Studying Liquid-Liquid Phase Separation and Biomolecular Condensates." *Cell* vol. 176,3 (2019): 419-434. doi:10.1016/j.cell.2018.12.035
58. Li, Qian; Wang, Xi; Dou, Zhihui; Yang, Weishan; Huang, Beifang; Lou, Jizhong; Zhang, Zhuqing (2020). *Protein Databases Related to LiquidâLiquid Phase Separation. International Journal of Molecular Sciences, 21(18), 6796–*. doi:10.3390/ijms21186796
59. Saleh, Omar A.; Jeon, Byoung-jin; Liedl, Tim (2020). *Enzymatic degradation of liquid droplets of DNA is modulated near the phase boundary. Proceedings of the National Academy of Sciences,202001654.* doi:10.1073/pnas.2001654117.

Acknowledgements: The authors thank T*yi*DE-Toronto, Canada for helping to write this manuscript.

Funding: The authors thank TCABS-E, Rajahmundry, India and T*yi*DE-Toronto, Canada for financial support.

Conflict of interest: This research article is an ongoing project currently at TCABS-E, Rajahmundry, India.

TCABSE-J Mini-Research Article
ISSN: 2583- 2557, *Volume 1, Issue 4, pp18-21. 2022.*

TCABSE-J
Interdisciplinary Sciences Journal

In vitro biological assay design for the inhibition of the matrix metalloproteinase, Collagenase type-1, using ethylenediaminetetraacetic acid, a metal ion chelator.

[1, 2, ⌘]Surya Ratnam V. Keerthi, [1, 2, ⌘]Jahnavi Chintalapati and [1, 3]Ravikiran S. Yedidi*

[1]The Center for Advanced-Applied Biological Sciences & Entrepreneurship (TCABS-E), Visakhapatnam 530016, AP; [2]Department of Biochemistry, [3]Department of Zoology, Andhra University, Visakhapatnam 530003, AP. ([⌘]These authors contributed equally) (*Correspondence to RSY: tcabse.india@gmail.com).

Coronavirus disease-2019 (COVID-19) has been a pandemic in recent years. The viral infection, mainly targeting the lungs, triggers inflammation in most cases leading to alveolar damage. The alveolar epithelial cells are especially prone to the viral infection-based inflammation related damage. Replenishment of these cells within a short period of time is very important for patients to recover which otherwise results in pulmonary disorders. Matrix metalloproteinases (MMPs) play a critical role in extracellular matrix remodeling during cellular regeneration. In this study, we used Collagenase type-1 enzyme which is also an MMP as a model enzyme to establish an enzyme inhibition assay that can be used to evaluate our newly designed MMP modulators. As a positive control, we used EDTA in this assay and evaluated the activity of Collagenase type-1 MMP in the presence and absence of EDTA using chicken liver tissue pieces. Our results suggest that EDTA indeed inhibits the enzyme activity of Collagenase type-1 MMP by chelating the metal ions in the buffer. Further the inhibitors will be evaluated in future using the EDTA as a positive control.

Keywords: Metalloproteinase, Collagenase type-1, EDTA, biological assay, enzyme inhibitors.

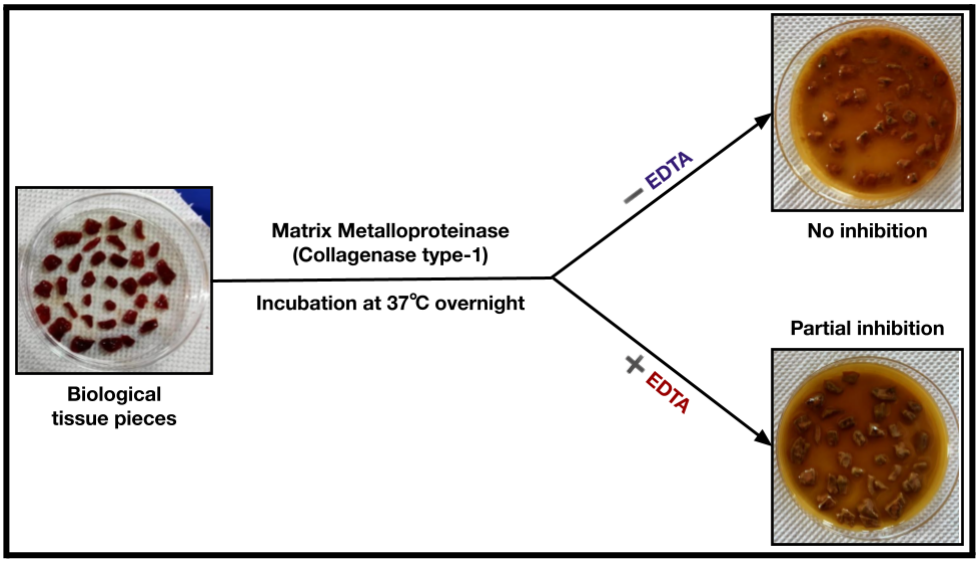

Figure 1. Overview of *in vitro* biological assay for Collagenase type-1, in the presence and absence of inhibitor, EDTA.

Citation: Keerthi, R., Chintalapati, J. and Yedidi, R. S. (2022). *In vitro* biological assay design for the inhibition of the matrix metalloproteinase, Collagenase type-1, using ethylenediaminetetraacetic acid, a metal ion chelator. *TCABSE-J*, Vol. 1, Issue 4:18-21. Epub: Oct5th, 2022.

Coronavirus disease-2019 (COVID-19) [1-9] causes severe damage to the alveolar epithelial cells in the lungs [10]. Infected patients, in order to recover faster, must not only be able to clear the viral load but also regenerate and replenish the damaged alveolar epithelium. However, during cellular regeneration replenishing the damaged tissue the remodeling of the extra -cellular matrix (ECM) is critical. In this context the matrix metalloproteinases (MMPs) are crucial in remodeling the extracellular matrix [11]. Recently we designed a novel strategy taking advantage of the MMPs and their tissue inhibitors of metalloproteinases (TIMPs) [12]. The equilibrium between MMPs and TIMPs is very important for healthy tissue remodeling which would otherwise result in scarring, fibrosis, cirrhosis, etc. [13-17].

There are several types of MMPs in humans that are secreted into the ECM. Collagenases (MMP-1, MMP-8, MMP-13, etc.), Gelatinases (gelatinase-A/MMP-2 and gelatinase-B/MMP -9) enzymes, Stromelysins (stromelysin-1/ MMP-3 and stromelysin-2/ MMP-10), Matrilysins (matrilysin-1/MMP-7 and matrilysin -2/MMP-26), Membrane type MMPs (MT-MMPs: MMP-14, MMP-15, MMP-16, MMP-24, MMP-17 and MMP-25), Other MMPs (MMP12, MMP19, MMP20, MMP22, MMP23, and MMP28). Within the MT-MMPs, some of them also have glycoprotein anchors to the membranes.

In this study, we focused on designing an *in vitro* biological assay to evaluate the MMP-1, Collagenase type-1 using chicken liver tissue pieces by using EDTA as a control. We hypothesized that MMP function is highly dependent on the metal ion binding which will be directly affected in the presence of EDTA. We performed the Collagenase type-1 assay in the presence and absence of EDTA to observe any difference in the activity of the MMP. If a difference is observed in this assay then, it can be fine tuned further to evaluate the potency of our MMP/TIMP modulators in future.

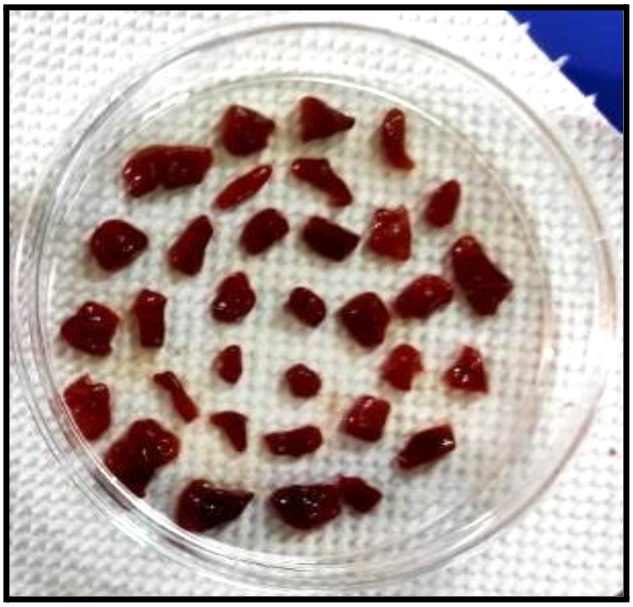

Figure 2. Sliced chicken liver pieces taken in a petri plate.

Materials & Methods:

NCBI search: An extensive search was performed using NCBI to identify different transcript variants of MMP-1. We identified two transcript variants of the human MMP-1 with the NCBI accession numbers: NM_002421.4 and NM_001145938.2 which were further used for any sequence information. The nucleotide sequences were further aligned to evaluate the presence of any significant differences between the two variants.

In vitro biological assay: Chicken liver pieces were used as tissue source to evaluate the enzyme activity in the presence and absence of EDTA. Two petri plates were sterilized with 70% ethanol and were labeled as plate 1 and plate 2. The chicken liver was sliced into small pieces and were taken equally into both the petri plates. To the petri plate 1, 8ml of 1x TAE buffer and 2ml of collagenase type-1 enzyme were added. To the petri plate 2, 8ml of 1x TAE buffer, 2ml of collagenase type-1 enzyme and 1ml of 0.5 M EDTA were added. Both the plates were put in the incubator at 37^0C overnight. After overnight incubation both the petri plates were observed for any changes.

ISSN: 2583- 2557, *Volume 1, Issue 4, pp18-21. 2022.*

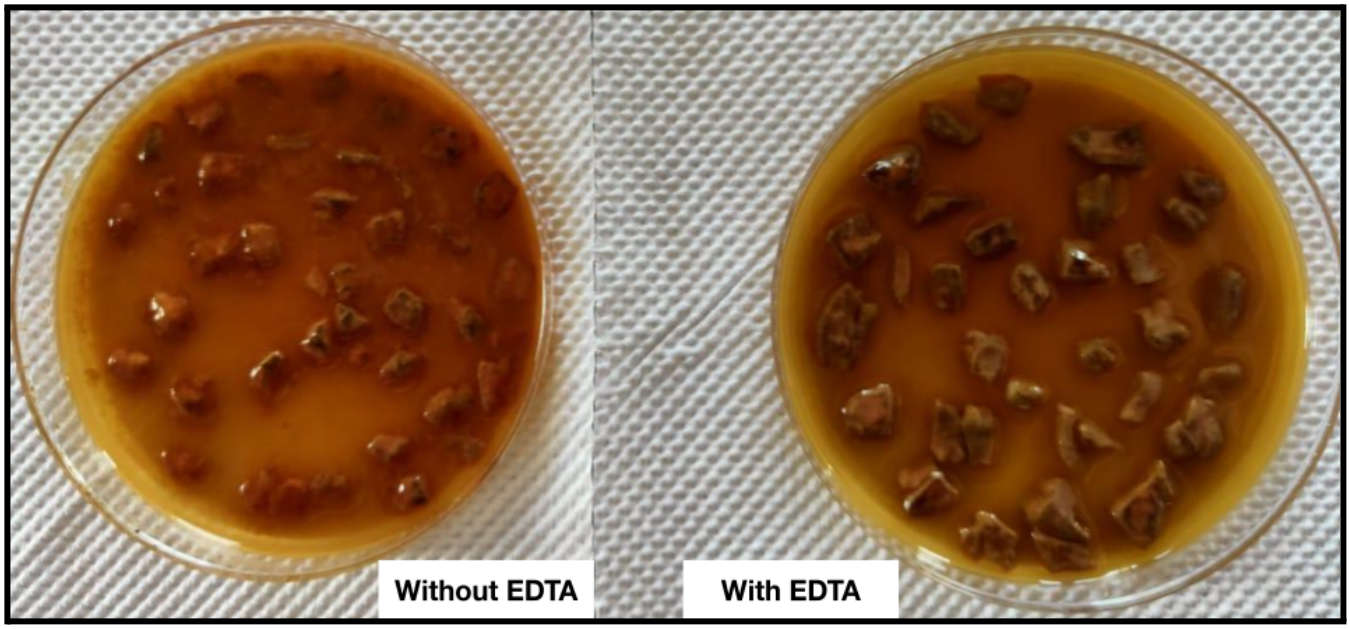

Figure 3. Post incubation observation of petri plates.

Results and Discussion:

In this assay, we demonstrated that Collagenase type-1 activity can be measured *in vitro* using chicken liver pieces both in the presence and absence of inhibitors such as EDTA. As shown in Figure 3, we can observe that in petri plate 1 (left plate) the Collagenase type-1 enzyme acts on the liver tissue based on notable deformation of the liver pieces along with the cloudiness of the buffer in the plate which is due to the activity of Collagenase type-1 on the extracellular matrix. Whereas in the case of petri plate 2 (right plate) we can observe due to the addition of EDTA the collagenase enzyme action is partially inhibited from the lack of significant deformation of the liver pieces. EDTA being a metal ion chelator acts as a sponge to chelate the metal ions in the buffer leading to the slowing down of the MMP activity. The resultant degraded tissue that is mixed with the buffer is further used to measure the optical absorbance at 600 nm. Further, by using the image quantification software such as the ImageJ, the pixels can be quantified along with the O.D. 600 nm. Such O.D. measurements can also be performed systematically for different time periods.

By using different doses of inhibitors one can establish dose-response curves that can further be used to calculate IC_{50} values of the inhibitors. In this way one can compare the potencies of various inhibitors. Thus, one can get a clear idea on the activity/inhibition of the MMPs in the presence and absence of the inhibitors with an appropriate control such as EDTA. This assay can thus be used in future to evaluate our in house MMP1 inhibitors.

References

1. Dhar Chowdhury S, Oommen AM. Epidemiology of COVID-19. *Journal of Digestive Endoscopy*. 2020;11(1):3-7. doi:10.1055/s-0040-1712187.
2. Hussin A Rothan, Siddappa N Byreddy. The epidemiology and pathogenesis of corona outbreak 2019. Journal of Autoimmunity. https://doi.org/10.1016/j.jaut.2020.102433.
3. A Du Toit, Outbreak of a novel corona virus, Nat.Rev.Microbiol.,18(123)(2020).
4. L.L.Ren, Y.M.Wang,Z.Q.Wu, Z.C.Xiang, L.Guo, T.Xu,et al. Identification of a novel coronavirus causing severe pneumonia in human a descriptive study. Chinese Med J(2020).
5. C. Huang, Y. Wang, X. Li, L. Ren, J. Zhao, Y.Hu et al. Clinical features of patients infected with 2019 novel coronavirus in Wuhan, China. Lancet, 395 (10223) (2020) pp. 495-506.
6. H.Lu . Drug treatment operations for the 2019 – new coronavirus (2019-nCoV). BioSci. Trends (2020).

7. W.Wang, J.Tang, F. Wei. Updated understanding of the outbreak 2019 novel coronavirus(2019-nCoV) in Wuhan, China. J.Med. Virol., 92(4)(2020), pp. 441-447.
8. H.Nishiura, S.M. Jung, N.M.Linton, R. Kinoshita, Y.Yang, K.Hayashi, *et al.* The extent of transmission of novel coronavirus in Wuhan, China, 2020. J.Clin Med.,9 (2020).
9. M. Basetti, A.Vena , D. Roberto Giacobbe. The Novel Chinese Coronavirus (2019-n- CoV) Infections: challenges for fighting the storm. Eur. J. Clin. Invest. (2020), Article e13209.
10. Chen, J., Wu, H., Yu, Y. *et al.* Pulmonary alveolar regeneration in adult COVID-19 patients. *Cell Res* **30,** 708–710 (2020).
11. Biological role of matrix metalloproteinases: a critical balance. S.Liffek, O. Schilly, W. Franke. European Respirator Journal 205. 360 191-208.
12. Buddana *et al.* (2021). Targeting the TIMPs with PROTAC-based small molecules as a potential therapeutic approach for Liver cirrhosis treatment. TCABSE-J, Vol. 1, Issue 1:9-11. Epub: Apr 13th , 2021.
13. Hideaki Nagase, Robert Visse, Gillian Murphy, Structure and function of matrix metalloproteinases and TIMPs, *Cardiovas -cular Research*, Volume 69, Issue 3, February 2006, Pages 562–573.
14. Newby A.C. Dual role of matrix metalloproteinases in intimal thickening and atherosclerotic plaque rupture. Physiol Rev 2005 85 131.
15. Spinale F.G.MMPs: regulation and dysregulation in the failing heart. Circ Res 2002 90 520 530.
16. Shah P.K. Inflammation, metalloproteinases and increased proteolysis an emerging pathophysiological paradigm in acute aneurysm. Circulation 1997 96 2115 2117.
17. Vissa R. Nagase H. MMPS and tissue inhibitors of metalloproteinases structure, Function and Biochemistry Circ Res 2003.

Acknowledgements: The authors thank T*yi*DE-Toronto, Canada for helping to write this manuscript. S.V.K. and J.C. thank Ms. Niharikha Mukala for chicken liver tissue.

Funding: The authors thank TCABS-E, Rajahmundry, India and T*yi*DE-Toronto, Canada for financial support.

Conflict of interest: This research article is an ongoing project currently at TCABS-E, Rajahmundry, India.

TCABSE-J Research Article
ISSN: 2583- 2557, *Volume 1, Issue 4, pp22-27. 2022.*

TCABSE-J Interdisciplinary Sciences Journal

Design of a pixel-based quantification method for *in vitro* colorimetric enzyme assay to evaluate enzyme inhibition in a dose-dependent manner.

[1, 2, #]Manasa Posimsetti, [1, 3, #]Sai Sritej Sanapala, [1, 4]Madhuri Vissapragada & [1, 5]Ravikiran S. Yedidi*

[1]The Center for Advanced-Applied Biological Sciences & Entrepreneurship (TCABS-E), Visakhapatnam 530016, AP; [2]Department of Biochemistry, [3]Department of Biotechnology, [4]Department of Human Genetics, [5]Department of Zoology, Andhra University, Visakhapatnam 530003, AP. ([#]These authors contributed equally) (*Correspondence to RSY: tcabse.india@gmail.com).

Biochemical and biophysical assays *in vitro* are often valuable assets to evaluate new compounds as inhibitors that can be developed into potential drugs. With rising expenses for laboratory research these days, designing an alternative economic method is highly desirable. In this study we evaluate the inhibitory potencies of two compounds, sodium azide (SA) and hydroxylamine (HA) in a dose-dependent manner using the standard horseradish peroxidase (HRP) enzyme. HRP is commonly conjugated to secondary antibodies that allows for colorimetric detection of proteins in western blotting technique. We chose to perform the colorimetric quantification using the pixel count with Image J software instead of the routine colorimetry/spectrophotometry. For both SA and HA the area under the curve (AUC) was quantified using the pixel count. Changes in the AUC with respect to the inhibitor concentration were carefully plotted to obtain the dose-dependent curves that were further used to calculate the individual potencies of SA and HA. This method was found to be at least 50 times more economical than the standard methods that use colorimetry/spectrophotometry.

Keywords: Colorimetry, HRP, enzyme inhibitors assay, pixel count, area under the curve, Image J.

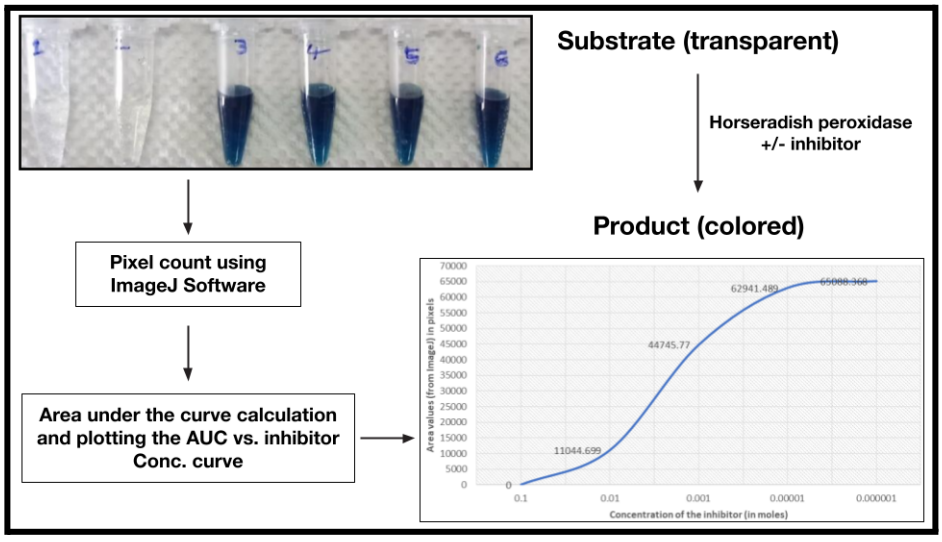

CC BY NC ND

Citation: Posimsetti, M., Sanapala, S. S., Vissapragada, M. and Yedidi, R. S. (2022). Design of a pixel-based quantification method for *in vitro* colorimetric enzyme assay to evaluate enzyme inhibition in a dose-dependent manner. *TCABSE-J*, Vol. 1, Issue 4:22-27. Epub: Oct5th, 2022.

Figure 1. Overview of the *in vitro* colorimetric enzyme assay quantification using pixel count to calculate inhibitor potency.

Enzyme kinetics are an integral part of many drug discovery programs in which candidate compounds (usually inhibitors of enzymes) are evaluated for their potency *in vitro* using biochemical assays and are ranked accordingly. Design of such assays is simple if a chromogenic or fluorescent substrate is available. Typically colorimeters and/or spectrophotometers are used to evaluate the absorbance of the reaction mixture at a given wavelength in the presence of various concentrations of inhibitor molecules. Drug discovery projects are often well funded. However, in startup companies and many academic laboratories, in order to generate preliminary data, one has to identify economic ways to evaluate the compounds towards preclinical drug discovery projects.

In this study we propose using the commonly used horseradish peroxidase (HRP) as a model enzyme along with a chromogenic substrate in the presence and absence of two HRP [1] inhibitors, sodium azide (SA) and hydroxylamine (HA). HRP is found in the roots of horseradish and is used extensively in biochemical applications. It is a metalloenzyme. It catalyzes the oxidation of various organic substrates by hydrogen peroxide [2-4]. HRP catalyzes the conversion of chromogenic substrates (e.g., TMB, DAB, ABTS) [5] into coloured products. The chromogenic substrate is expected to yield different shades of green depending on the inhibitor concentration.

In order to quantify the color change, we used the ImageJ software [6-8] that can quantify the pixels in the image. High resolution camera was used to take the pictures of the reaction mixtures containing various concentrations of either SA or HA. Once the pixels were read in, the area under the curve (AUC) was calculated for each measurement. These AUC values were then plotted against the inhibitor concentrations in order to determine the enzyme inhibition. We further made an attempt to calculate the 50% inhibitory concentrations (IC_{50}s) for both SA and HA. Our method completely bypasses the usage of colorimeter and/or spectrophotometer thus making this method more economical.

Figure 2. Sliced chicken liver pieces taken in a petri plate.

Materials & Methods:

Preparation of stock solutions for inhibitors: In this study, 2 inhibitors which inhibit the enzyme HRP were considered namely, Sodium azide & Hydroxylamine. Six different concentrations/ dilutions of stock solution of both inhibitors i.e., 0.1M, 10mM, 1mM, 100µM, 10µM & 1µM are needed for the enzyme assay. For this, two concentrations i.e., 1M & 1mM stock solutions, 1ml of each of both the inhibitors are prepared. To prepare 1ml of 1M solution, the given formula is used:

$$M = \frac{wt\ (gm)}{Mol.Wt.} \times \frac{1000}{Vol\ (ml)}$$

For example, in the case of Sodium Azide (molecular weight: 65.01) the total weight required was calculated to be 0.065 grams in order to prepare a stock solution of 1M concentration and 1ml volume. Similarly, a 1ml stock solution of 1M hydroxylamine was also prepared by weighing the required amount of the inhibitor and dissolving it in deionized water. Further dilutions were made in order to obtain the required concentrations of each inhibitor.

Preparation of Substrate & Enzyme: The substrate is prepared by mixing 10ml of ABTS (2,2'-azino-bis(3-ethylbenzothiazoline-6-sulfonic acid)) with 2µl of hydrogen peroxide. Five ml of horseradish peroxidase (HRP) enzyme is taken.

Colorimetry-based Enzyme Assay: The total reaction mixture volume i.e., substrate + enzyme + inhibitor + distilled water should be 300µl in volume. The volumes of substrate (269µl), enzyme (1µl) and the inhibitor (30µl) remain the same. A total of 6 different concentrations of inhibitors are prepared.

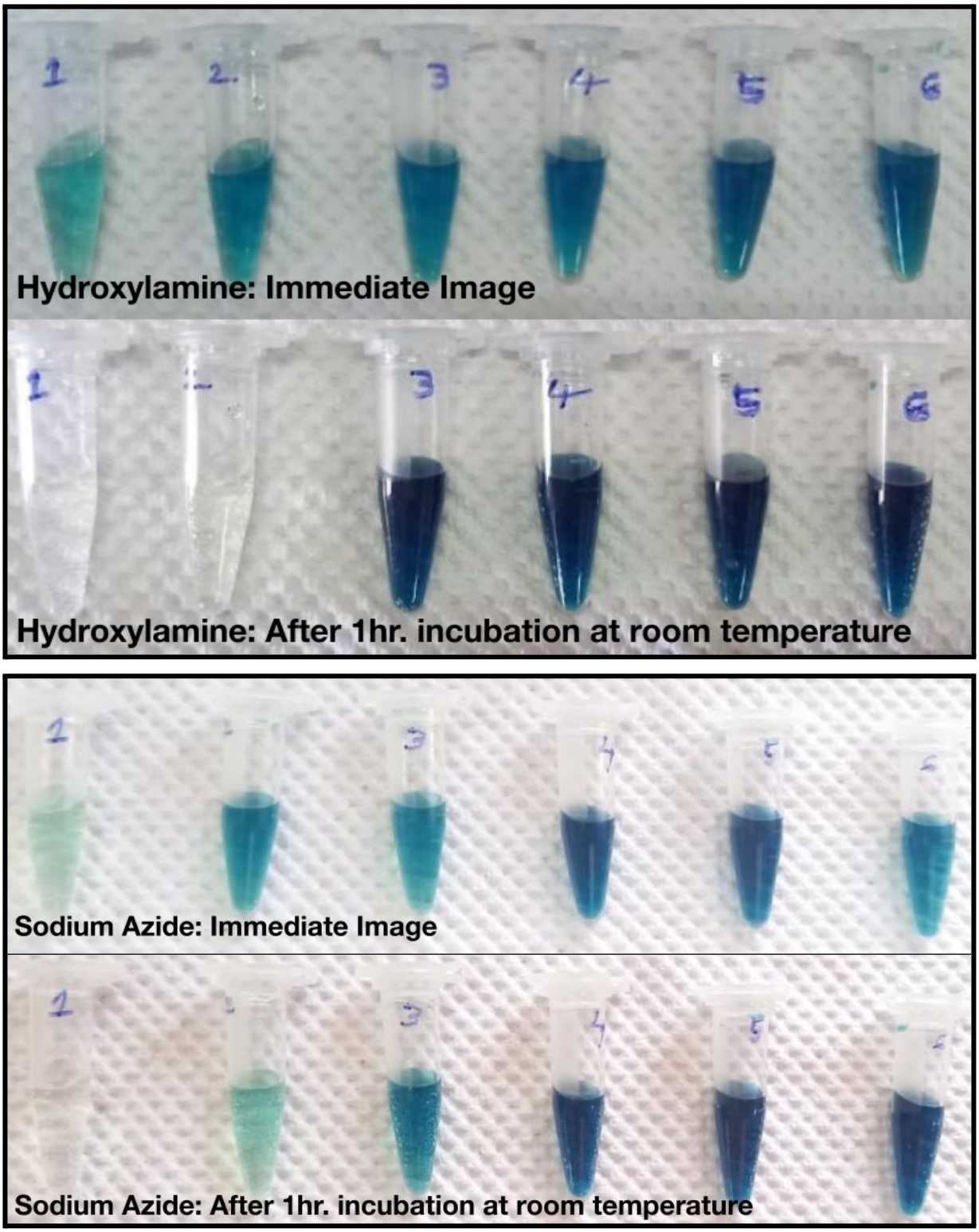

Figure 2. Reaction tubes showing different shades of green.

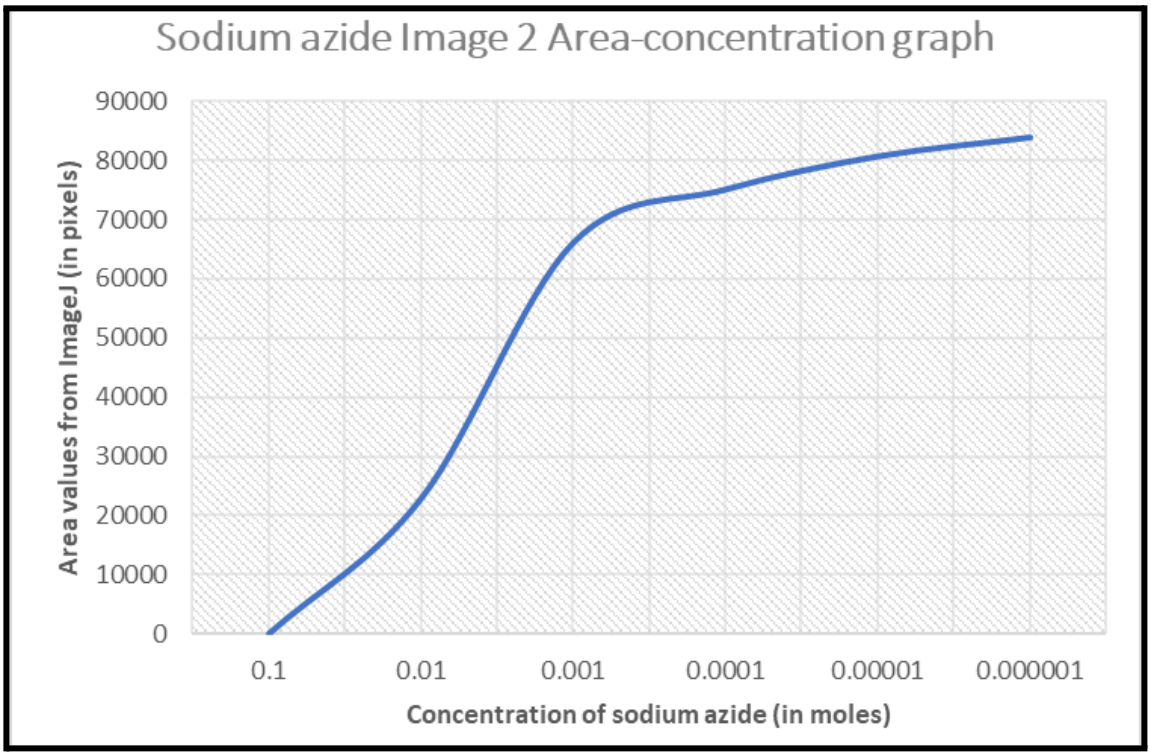

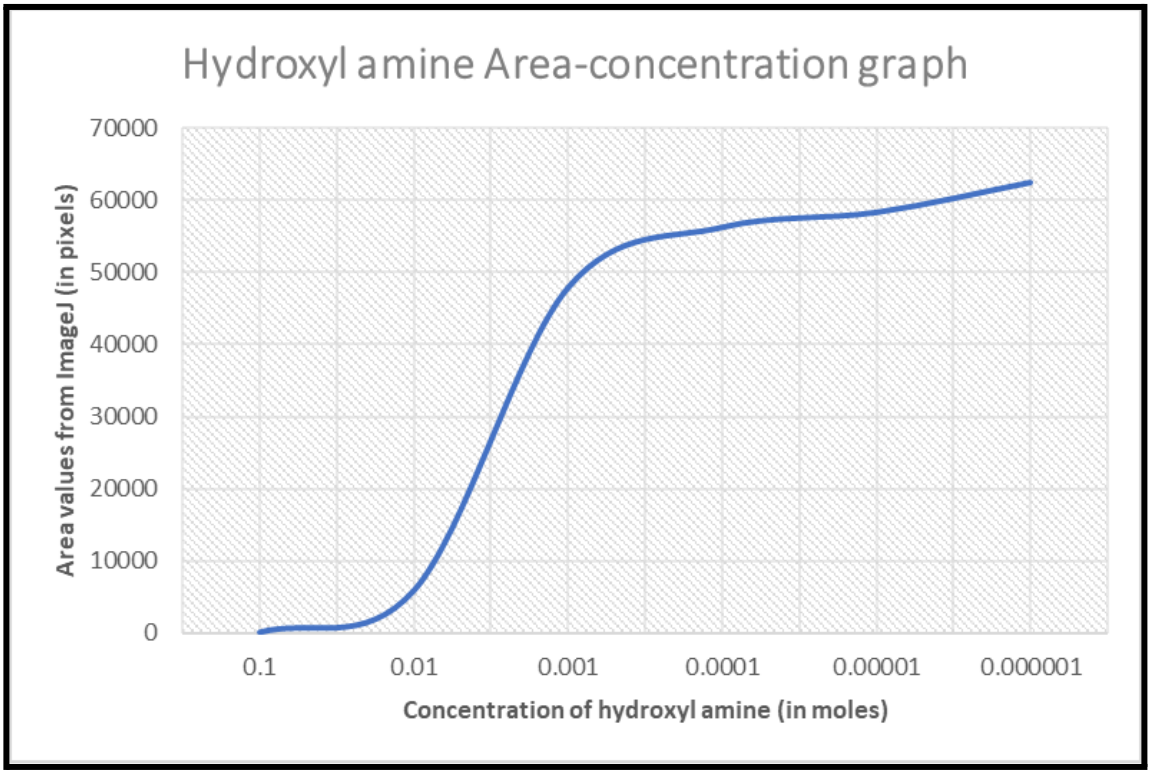

Figure 3. AUC vs. [I] curve plotted for 6 different values.

Six polypropylene tubes of 2ml capacity were taken for the 5 different concentrations of the inhibitors, 0.1M, 0.01M, 0.001M, 0.0001M, 0.00001M & 0.000001M. These 6 concentrations were chosen to obtain a clear inhibition curve of the enzyme activity that would be helpful in calculating the IC_{50} values. Using a micropipette, substrate is added first into all the tubes. Following it, deionized water is added into the tubes. Next, the enzyme is added into each of the tubes. The inhibitor is added in the last into all the tubes according to the values given in the above table. After adding all these, an immediate image is taken. Then, the tubes were incubated for 1 hour at room temperature. After incubation, another image is taken to determine the color change. This process is performed for both the inhibitors in similar manner. Repeats were performed in order to obtain at least two values for each.

Pixel quantification using ImageJ software: ImageJ is a Java-based image processing program developed at the National Institutes of Health and the Laboratory for Optical and Computational Instrumentation (LOCI, University of Wisconsin). It can display, edit, analyze, process, save, and print 8-bit color and grayscale, 16-bit integer, and 32-bit floating point images. It can calculate area and pixel value statistics. It can measure distances and angles. Using Image J, enzyme activity is determined based on color intensity & pixel values. Image J application is opened and image is selected and uploaded. After uploading the image, a rectangle tool is selected and a solution containing the area in each tube in the image is outlined using the tool. To do this, "Analyze" option is selected and in the "gels" option, "select first lane" option is clicked. Then, after selecting the 2nd tube, "select next lane" option is clicked and so on. After selecting all the tubes, go to "Analyze" & "gels" & then click "Plot Lanes". After obtaining the plots, using the "Straight" tool, the curve area is plotted. Then, "Wand" tool is used to select the area of the plot and measure it.

Results and Discussion:

Colorimetric enzyme assay: The images of all tubes before incubation and after incubation were compared to see any changes in the color for both inhibitors. As shown in Figure 2, the color change was observed in the first tube where the highest tested concentration of HA was present compared to the other tubes. Similar trend was observed for SA as well. With decreasing inhibitor concentrations in both cases (SA and HA) the green color was more intense indicating the increased activity of the HRP in the presence of lower concentrations of inhibitor. The colors were further quantified using imageJ.

Inhibitory potencies of SA and HA: The IC_{50} values for both SA and HA were arbitrarily calculated from the curves plotted through manual inspection of the curves with the help of MS-Excel sheets. In each case, the corresponding AUC value was considered for each concentration point of the inhibitors. In the case of SA, the two experiments yielded 5.25 mM and 6.0 mM IC_{50} values of HRP. Hence the average of both experiments including the standard deviation was calculated to be: 5.625 mM $\pm$ 0.53. Similarly, the two values for HA evaluation were used to obtain a final average IC_{50} value of 4.25 mM $\pm$ 2.0. Based on the standard deviation values for both SA and HA, we conclude that this assay can further be used to evaluate inhibitors of other enzymes that act on chromogenic substrates.

Applications of this method in future: The current study evaluates SA and HA at 6 different concentrations using HRP as a model system in the presence of ABTS substrate. This economical method is very much useful especially when HRP is cloned in frame with other enzymes such as PETase in plastic degradation analysis. Further, this assay can also be used to design to test the environment pollutants that can be detected by using HRP without the requirement of colorimeter and/or spectrophotometer. Especially for field

studies, miniaturization of this assay would significantly help because one can simply quantify the pixels instantaneously without any waiting period for data acquisition and/or analysis.

References:

1. Gajhede M, Schuller DJ, Henriksen A, Smith AT, Poulos TL (December 1997). "Crystal structure of horseradish peroxidase C at 2.15 A resolution". *Nature Structural Biology*. 4 (12): 1032–8.
2. Veitch NC (February 2004). "Horseradish peroxidase: a modern view of a classic enzyme". *Phytochemistry*. 65 (3): 249–59.
3. Akkara JA, Senecal KJ, Kaplan DL (October 1991). "Synthesis and characterization of polymers produced by horseradish peroxidase in dioxane". *Journal of Polymer Science*. 29 (11): 1561–74.
4. Beyzavi K, Hampton S, Kwasowski P, Fickling S, Marks V, Clift R (March 1987). "Comparison of horseradish peroxidase and alkaline phosphatase-labelled antibodies in enzyme immunoassays". *Annals of Clinical Biochemistry*. 24 (Pt 2) (2): 145–52.
5. Bourbonnais, Robert; Leech, Dónal; Paice, Michael G. (1998-03-02), "Electrochemical analysis of the interactions of laccase mediators with lignin model compounds", *Biochimica et Biophysica Acta (BBA) - General Subjects*, 1379 (3): 381–390
6. Schneider, C. A., Rasband, W. S., & Eliceiri, K. W. (2012). NIH Image to ImageJ: 25 years of image analysis. *Nature Methods*, *9*(7), 671–675.
7. Schindelin, J., Rueden, C. T., Hiner, M. C., & Eliceiri, K. W. (2015). The ImageJ ecosystem: An open platform for biomedical image analysis. *Molecular Reproduction and Development*, *82*(7–8), 518–529.
8. Rueden, C. T., Schindelin, J., Hiner, M. C., DeZonia, B. E., Walter, A. E., Arena, E. T., & Eliceiri, K. W. (2017). ImageJ2: ImageJ for the next generation of scientific image data. *BMC Bioinformatics*, *18*(1).

Acknowledgements:

The authors thank T*yi*DE-Toronto, Canada for helping to write this manuscript.

Funding:

The authors thank TCABS-E, Rajahmundry, India and T*yi*DE-Toronto, Canada for financial support.

Conflict of interest: This research article is an ongoing project currently at TCABS-E, Rajahmundry, India.

TCABSE-J Research Article
ISSN: 2583- 2557, *Volume 1, Issue 4, pp28-34. 2022.*

TCABSE-J
Interdisciplinary Sciences Journal

Testing the feasibility of using the common laboratory strain *E. coli* DH5α as a model system to study clarithromycin-resistance in *Helicobacter pylori*

[1, 2, #]Vineela R. D. Nerusu, [1, #]Madhumita Aggunna & [1, 3]Ravikiran S. Yedidi*

[1]The Center for Advanced-Applied Biological Sciences & Entrepreneurship (TCABS-E), Visakhapatnam 530016, AP; [2]Department of Applied Microbiology, Sri Padmavathi Mahila Visvavidyalayam, Tirupati 517502; [3]Department of Zoology, Andhra University, Visakhapatnam 530003, AP. ([#]These authors contributed equally) (*Correspondence to RSY: tcabse.india@gmail.com).

Antimicrobial-resistance (AMR) has emerged as a leading research field these days with an increasing number of drug-resistant microbes such as *Helicobacter pylori*. Most of the bacterial strains these days have evolved and developed resistance to a broad range of antibiotics of different classes resulting in AMR. *H. pylori* is the primary cause for the microbial infection-related gastric ulcers and sometimes cancers as well. Clarithromycin is a classical old generation antibiotic that lost its potency against the drug-resistant bacteria due to base substitutions in its target, the 23S ribosomal RNA. In this study we performed an extensive Bioinformatics analysis of the 23S rRNA sequence from *H. pylori* strains that are resistant to clarithromycin (Cly^r). In parallel we compared the 23S rRNA sequence of *E. coli* strains K-12 and DH5α that are commonly used in the laboratories with the wild type and mutant strains of *H. pylori* with a goal to evaluate Cly^r using the *E. coli* strains to circumvent the process of obtaining clinical patient samples of *H. pylori* which is often challenging administratively, ethically and legally. We evaluated the growth of DH5α strain in the presence of various concentrations of clarithromycin.

Keywords: *Helicobacter pylori*, gastric ulcers, DH5α, antimicrobial-resistance, clarithromycin-resistance.

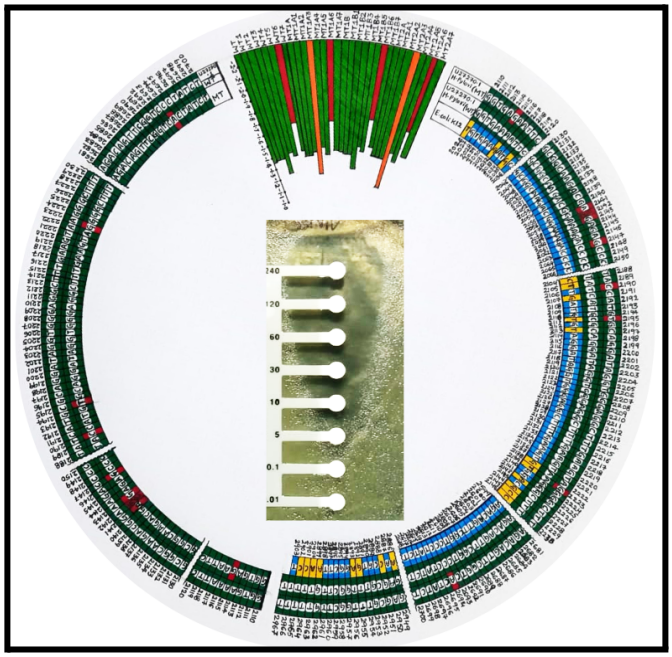

Figure 1. Circular plot showing the sequence alignment of *H. pylori* wild type vs. mutants (left semicircle) and *H. pylori* vs. *E. coli* (right semicircle). *H. pylori* mRNA stability for wild type vs. mutants (top of the circle). Clarithromycin activity discs in the middle are placed in the *E. coli* DH5α plate.

CC BY NC ND

Citation: Nerusu, V. R. D., Aggunna, M. and Yedidi R. S. (2022). Testing the feasibility of using the common laboratory strain *E. coli* DH5α as a model system to study clarithromycin-resistance in *Helicobacter pylori*. *TCABSE-J*, Vol. 1, Issue 4:28-34. Epub: Oct5th, 2022.

TCABSE-J Research Article
ISSN: 2583- 2557, *Volume 1, Issue 4, pp28-34. 2022.*

Helicobacter pylori infected nearly more than 50% of the world population and it is mainly in developing countries (80%). In the past decade, the total number of cases was more than 4 billion. Gastritis, the inflammation of gastric mucosal lining could be acute or chronic. *H. pylori* has been known to cause non-erosive gastritis where the mucosal lining is still intact. However, the infection can be severe sometimes resulting in gastric ulcers and even cancer. Ulcers are formed generally in the stomach and proximal duodenum. *H. pylori* generally weakens the mucous coating of the stomach so that the inner layer is exposed to acid resulting in sores formation. These sores often lead to the formation of peptic ulcers. More than 60% of the gastric cancer cases are due to the infections by *H. pylori*.

Typically the current treatment regimens for *H. pylori* infections include combination of antibiotics (amoxicillin, clarithromycin, metroni -dazole, tetracycline, tinidazole, levofloxacin, rifabutin); acid production inhibitors (dexlan -soprazole, esomeprazole, lansoprazole, omepra -zole, pantoprazole, rabeprazole); bismuth subsalicylate and antihistamine drugs (cimeti -dine, famotidine, Pepcid, nizatidine). However, mutations in the drug targets of *H. pylori* lead to antibiotic-resistance. In the case of amoxicillin, mutations in the penicillin binding protein (PBP) lead to reduced accumulation of amoxicillin in the cell; mutations in the NADPH oxidoreductase lead to resistance against the DNA damaging agent metronidazole; due to mutations in the bacterial DNA gyrase levofloxacin-resistance occurs; either single or combination of mutations in the 16S rRNA of the ribosomal 30S subunit confer resistance against tetracycline while clarithromycin -resistance (Cly^r) arises due to mutations in the 23S rRNA.

In this study, we focused on evaluating the Cly^r using the commonly used laboratory strain of *E. coli*, DH5α. Clarithromycin is a semi -synthetic macrolide antibiotic that targets the bacterial 23S rRNA. Mutations with base substitutions such as A2142C, A2142G and A2143G in the 23S rRNA were primarily shown to be responsible for Cly^r in *H. pylori*. Other 23S rRNA mutations in *H. pylori* that are responsible in combination with the above mentioned are A2115G, G2141A, C2147G, T2190C, C2195T, A2223G and C2694A. Extensive sequence alignments were performed to evaluate the homology between the 23S rRNA molecules of *H. pylori* and *E. coli*, DH5α.

Materials & Methods:

NCBI Search: NCBI search was used for accession no: U27270.1 (23S rRNA and 5S rRNA of *Helicobacter pylori*) and also search for 23S rRNA of *E. coli* DH5-α (accession no: CP025520.1). The FASTA sequences from 372 to 3339 in *H. pylori* (accession no: u27270.1) and 3023394 to 3026311 in *E.coli* DH5α (accession no: CP025520.1) were identified as the coding sequence for 23S rRNA and were aligned using NCBI global align algorithm. Similarly the 23S rRNA sequence of *H. pylori* was aligned with the sequence of *E. coli* K-12 (PDB ID: 4V69) of 2903 length due to lack of a three-dimensional structure for *E.coli* DH5α 23S rRNA using NCBI global align algorithm.

RNA FOLD: Vienna RNAfold (http://rna.tbi.univie.ac.at/cgi-bin/RNAWebSuite/RNAfold.cgi) is a server-based open source software package that calculates the secondary structures of RNA sequences with a limitation of 7,500 nucleotides for partition function calculation and 10,000 nucleotides for minimum energy predictions. The wild type FASTA sequence (accession no: U27270.1) was used for building the RNA secondary structure and predicting its energy value. In order to download the image the online image converter (view in forna) was chosen in the download options. The image was then downloaded and saved in the PNG form.

Multiple sequence alignment: Clustal omega is the alignment software that helps to align three or more sequences up to align about 4000 sequences https://www.ebi.ac.uk/Tools/msa/clustalo/.

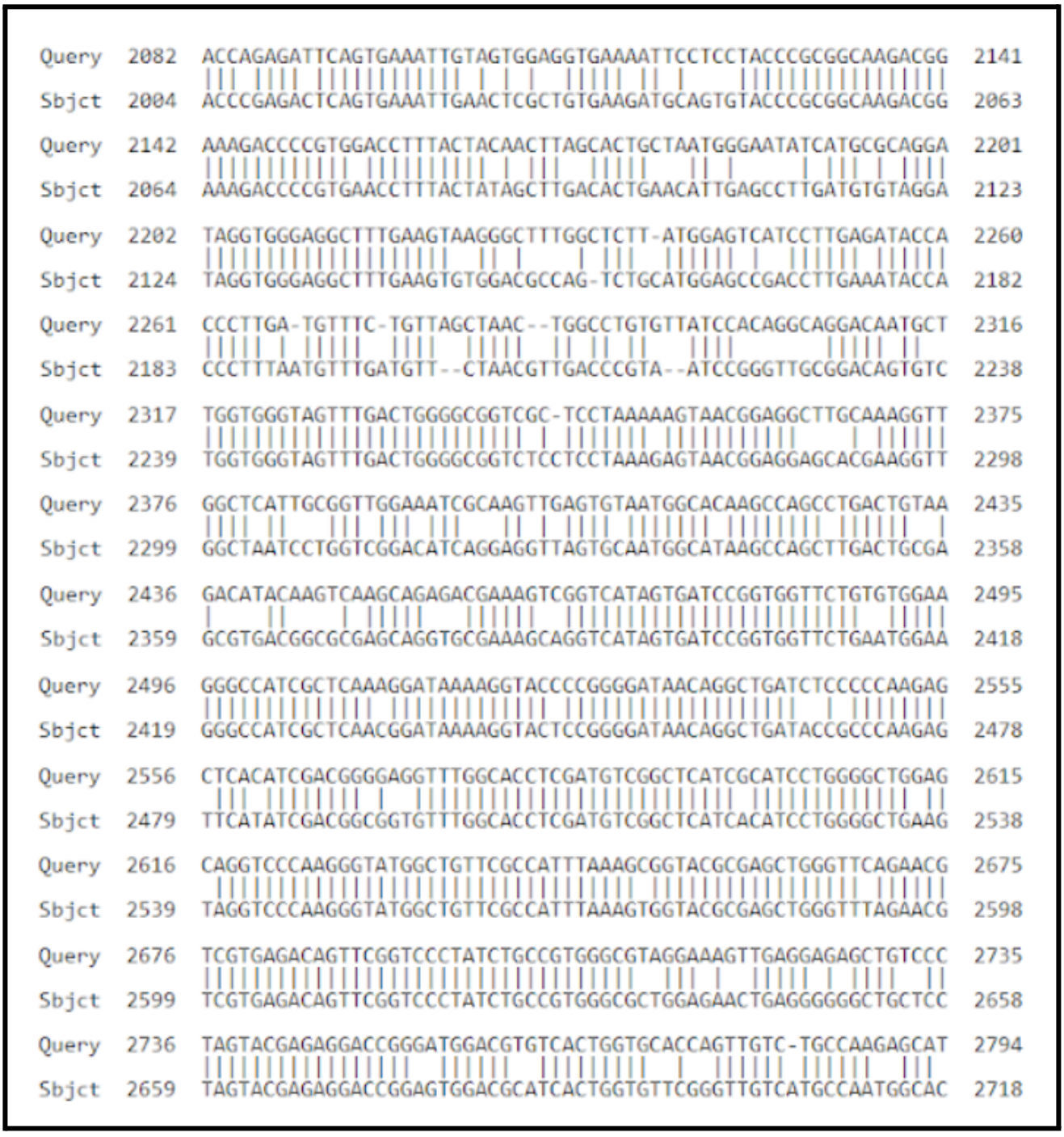

Figure 2. *H. pylori* vs. *E. coli* DH5α 23S rRNA alignment.

The sequence alignment was done for 23s ribosomal RNA sequences of *E.coli* DH5α and *H. pylori*.

Preparation of LB-Agar plates: In a clean bottle, 6.25gms of Luria Bertani powder and 3.75gms of agar powder were weighed to which 250ml of water was added and mixed well. Then it was autoclaved at 121℃, 15lbs pressure for 20minutes.

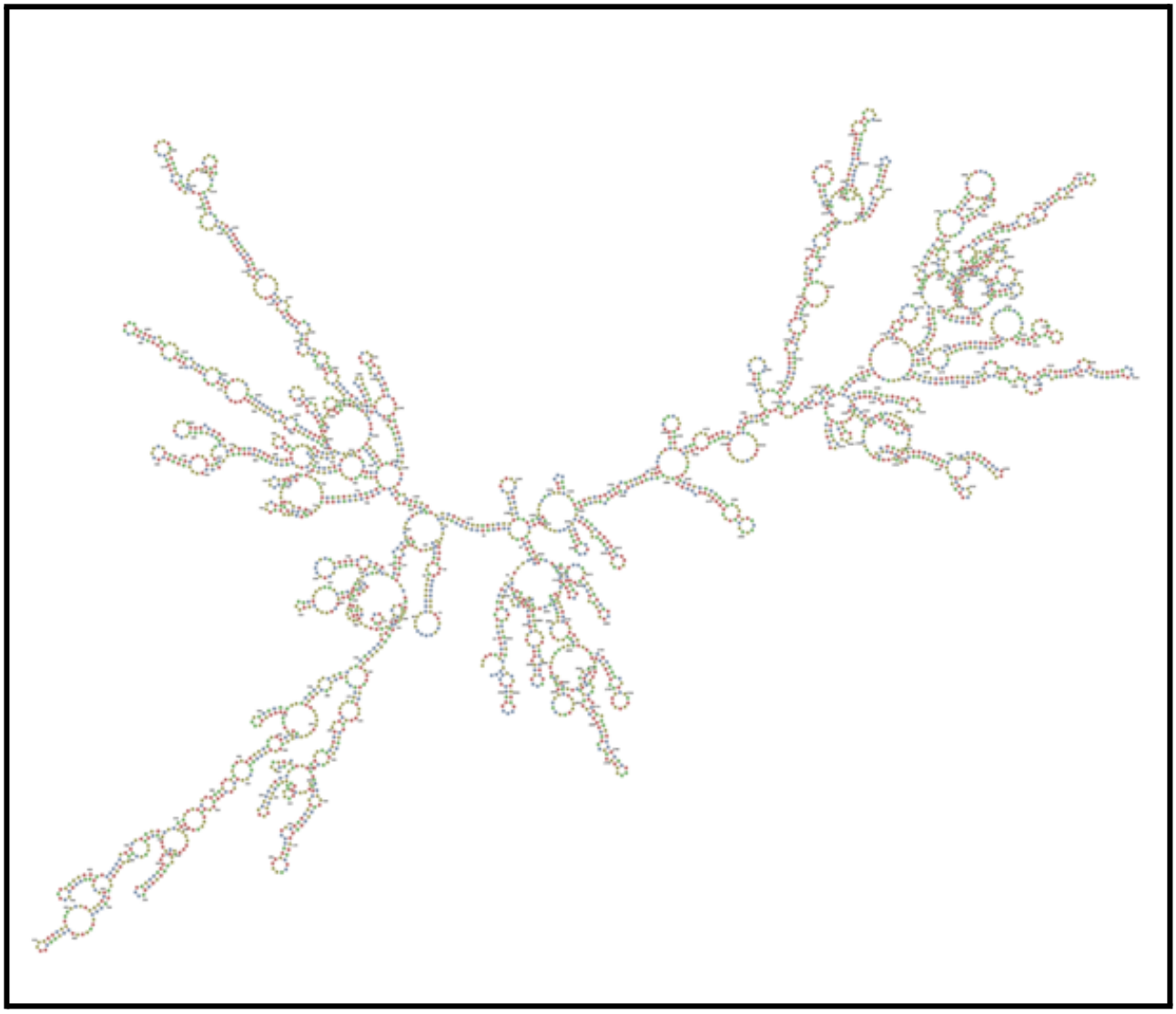

Figure 3. Predicted structure of *H. pylori* 23S rRNA.

The sterile petri plates were taken and media poured into them and allowed to solidify.

Antibiotic sensitivity test: Strips of clarithromycin of different concentrations were taken. Strip A has a concentration range of 0.01 to 240 micrograms and strip B of concentration 0.001 to 16 micrograms. *E.coli* DH5-α cell suspension was taken. Two prepared LB media plates were taken, 50 microliters of *E.coli* DH5-α cells were added to either plate. One LB plate was kept as negative control i.e., no addition of *E.coli*. Strip A of clarithromycin was placed in one plate and strip B in another plate. Incubate three plates at 37℃ for 16 hours.

Results and Discussion:

Bioinformatics: NCBI Search: To use *E. coli* DH5-α (accession number: CP025520.1) instead of *H. pylori* (accession no: U27270.1) for laboratory work their sequences are compared using global align to know their similarity (Figure 2). An overall 69% sequence homology was observed between the 2 which was considered as reasonable to consider the *E. coli* DH5-α as a model organism

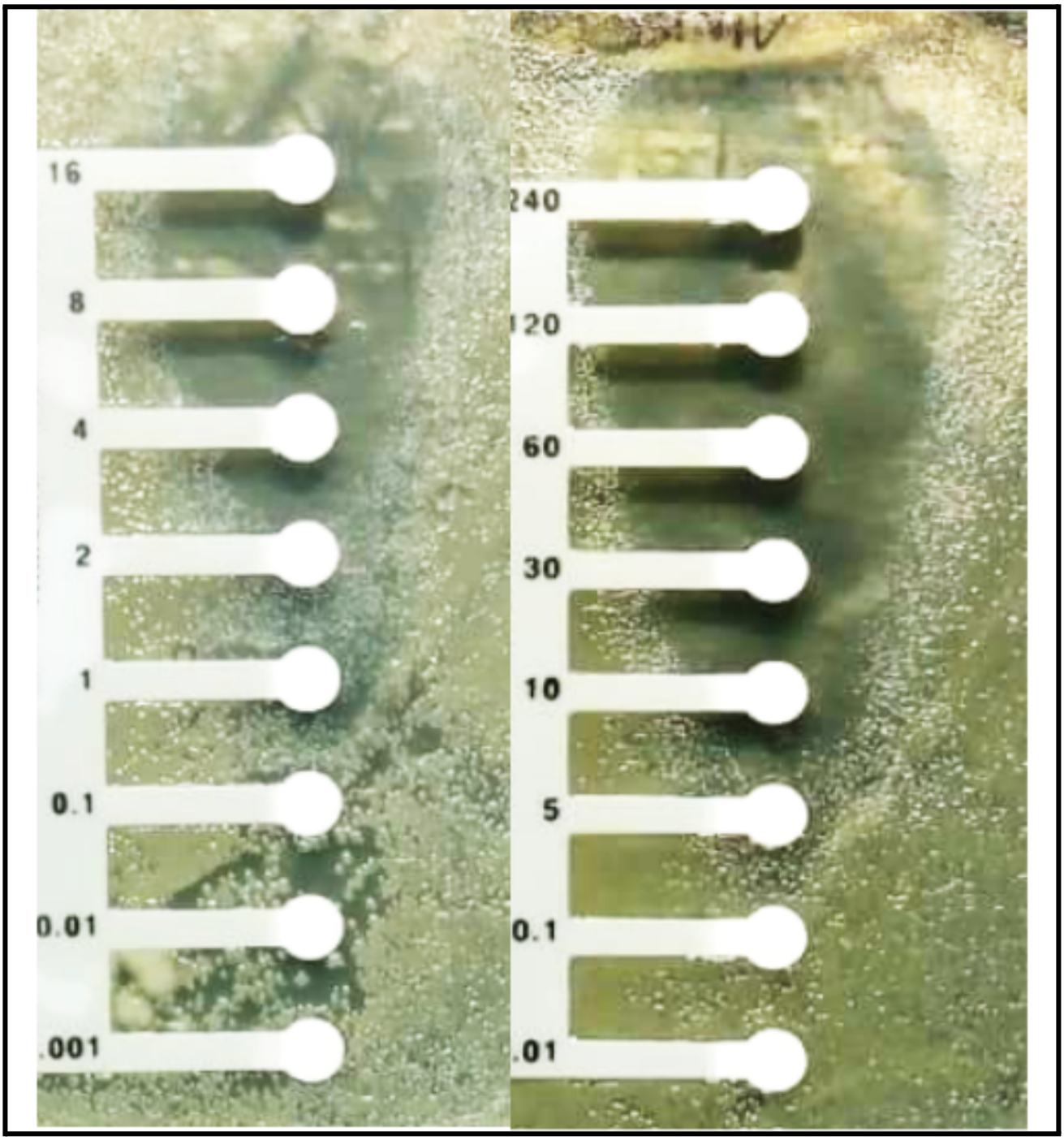

Figure 4. Clarithromycin sensitivity test for *E. coli* DH5α cells.

to study in the laboratory instead of *H. pylori* because *H. pylori* requires access to human clinical samples that require clearances from various departments such as ethical, clinical, research, etc. As shown in Figure 2, the overall sequence alignment looks good.

RNA secondary structures: Mutations in 23sribosomal RNA of *Helicobacter pylori* as

mentioned in introduction, mutations that provide resistance to clarithromycin in *H. pylori* are A2142G/C, A2143G, G2141A, C2147G, T2190C, C2195T ,A2223G, C2694A, A2115G. Secondary structures for all mutants including the wild type were predicted using RNAfold. Seven wild types are created by placing one mutation at a time in wild type sequence except A2142G/C and A2143G and they are labeled as WT1, WT2, WT3, WT4, WT5, WT6, WT7 and original wild type as WT. Taking A2142G, A2142C, A2143G as major mutations, remaining mutants were added one after one along with them, named as MT1A(A2142G), MT1B(A2142C), MT2A(A2143G). The mutations in MT1A(A2142G) group are MT1A1(A2142G, G2141A), MT1A2(A2142G, C2147G), MT1A3(A2142G, T2190C), MT1A4(A2142G, C2195T), MT1A5(A2142G, A2223G), MT1A6(A2142G, C2694A), MT1A7(A2142G, A2115G). The mutations in MT1B(A2142G) group are: MT1B1(A2142C, G2141A), MT1B2(A2142C, C2147G), MT1B3(A2142C, T2190C), MT1B4(A2142C, C2195T), MT1B5(A2142C, A2223G), MT1B6(A2142C, C2694A), MT1B7(A2142C, A2115G). The mutations in MT2A (A2143G) group are: MT2A1(A2143G, G2141A), MT2A2(A2143G, C2147G), MT2A3(A2143G, T2190C), MT2A4(A2143G, C2195T), MT2A5(A2143G, A2223G), MT2A6(A2143G, C2694A), MT2A7(A2143G, A2115G). The total number of mutations are 32. Minimum free energy, ensemble diversity and AMFE values of different mutations given by RNA Fold were plotted as shown in Figure 1. The overall AMFE values of the mutants are within the range of the wild type suggesting that these mutations are only affecting the clarithromycin-resistance but not the overall stability of the predicted secondary structures of the RNAs.

Clarithromycin activity test: This test was performed with the *E. coli* DH5-α strain of cells. The zones of inhibition for *E.coli* DH5-α cells to clarithromycin are given below:

[Clarithromycin]	Zone of inhibition
1 mcg	0.6cm
4mcg	2cm
8 mcg	1.7cm
16 mcg	2.8cm
120mcg	3.6cm
240mcg	3.9cm

Based on the zones of inhibition, we calculated the minimum inhibitory concentration of clarithromycin as 8 mcg. In future, this value will be compared to the mutant strains that show clarithromycin-resistance.

The current study focused on using the *E.coli* DH5-α cells as a model to study Cly^r seen in *H. pylori* human clinical samples. By establishing this model, one can speed up the process of studying the Cly^r using simple laboratory bacterial strains instead of going through complicated ethical, clinical and administrative guidelines and challenges involved. However, the complete model development is beyond the scope of this report and shall be continued in the future.

References

1. Clinical Microbiology Reviews, 0893-8512/97/$04.0010 Oct. 1997, p. 720–741 Vol. 10, No. 4 Copyright © 1997, American Society for Microbiology *Helicobacter pylori* Bruce E. Dunn,1,2* Hartley Cohen,3 and Martin J. Blaser 4,5.
2. Kusters, J. G., van Vliet, A. H., & Kuipers, E. J. (2006). Pathogenesis of Helicobacter pylori infection. *Clinical microbiology reviews*, *19*(3), 449–490. https://doi.org/10.1128/CMR.00054-05.
3. Baj, J., Forma, A., Sitarz, M., Portincasa, P., Garruti, G., Krasowska, D., & Maciejewski, R. (2020). *Helicobacter pylori* Virulence Factors-Mechanisms of Bacterial Pathogenicity in the Gastric Microenvironment. *Cells*, *10*(1), 27. https://doi.org/10.3390/cells10010027.

4. Chmiela, M., & Kupcinskas, J. (2019). Review: Pathogenesis of Helicobacter pylori infection. *Helicobacter*, *24 Suppl 1*(Suppl Suppl 1), e12638. https://doi.org/10.1111/hel.12638.
5. Yang, J. C., Lu, C. W., & Lin, C. J. (2014). Treatment of Helicobacter pylori infection: current status and future concepts. *World journal of gastroenterology*, *20*(18):5283–5293. https://doi.org/10.3748/wjg.v20.i18.5283.
6. Hooi, J., Lai, W. Y., Ng, W. K., Suen, M., Underwood, F. E., Tanyingoh, D., Malfertheiner, P., Graham, D. Y., Wong, V., Wu, J., Chan, F., Sung, J., Kaplan, G. G., & Ng, S. C. (2017). Global Prevalence of Helicobacter pylori Infection: Systematic Review and Meta-Analysis. *Gastroenterology*, *153*(2), 420–429. https://doi.org/10.1053/j.gastro.2017.04.022.
7. Kouitcheu Mabeku, L. B., Noundjeu Ngamga, M. L., & Leundji, H. (2018). Potential risk factors and prevalence of Helicobacter pylori infection among adult patients with dyspepsia symptoms in Cameroon. *BMC infectious diseases*, *18*(1), 278. https://doi.org/10.1186/s12879-018-3146-1.
8. Munita, J. M., & Arias, C. A. (2016). Mechanisms of Antibiotic Resistance. *Microbiology spectrum*, *4*(2), 10.1128/microbiolspec.VMBF-0016-2015. https://doi.org/10.1128/microbiolspec.VMBF-0016-2015
9. Francesco, V. D., Zullo, A., Hassan, C., Giorgio, F., Rosania, R., & Ierardi, E. (2011). Mechanisms of Helicobacter pylori antibiotic resistance: An updated appraisal. *World journal of gastrointestinal pathophysiology*, *2*(3), 35–41.
10. Nishizawa, T., & Suzuki, H. (2014). Mechanisms of Helicobacter pylori antibiotic resistance and molecular testing. *Frontiers in molecular biosciences*, *1*, 19.
11. Kim, S. Y., Joo, Y. M., Lee, H. S., Chung, I. S., Yoo, Y. J., Merrell, D. S., & Cha, J. H. (2009). Genetic analysis of Helicobacter pylori clinical isolates suggests resistance to metronidazole can occur without the loss of functional rdxA. *The Journal of antibiotics*, *62*(1), 43–50.
12. Marques, A. T., Vítor, J., Santos, A., Oleastro, M., & Vale, F. F. (2020). Trends in *Helicobacter pylori* resistance to clarithromycin: from phenotypic to genomic approaches. *Microbial genomics*, *6*(3), e000344.
13. Roszczenko-Jasińska, P., Wojtyś, M. I., & Jagusztyn-Krynicka, E. K. (2020). Helicobacter pylori treatment in the post-antibiotics era-searching for new drug targets. *Applied microbiology and biotechnology*, *104*(23), 9891–9905.
14. Agudo, S., Pérez-Pérez, G., Alarcón, T., & López-Brea, M. (2010). High prevalence of clarithromycin-resistant Helicobacter pylori strains and risk factors associated with resistance in Madrid, Spain. *Journal of clinical microbiology*, *48*(10), 3703–3707.
15. Hussein, R. A., Al-Ouqaili, M., & Majeed, Y. H. (2022). Detection of clarithromycin resistance and 23SrRNA point mutations in clinical isolates of *Helicobacter pylori* isolates: Phenotypic and molecular methods. *Saudi journal of biological sciences*, *29*(1), 513–520.
16. Albasha, A. M., Elnosh, M. M., Osman, E. H., Zeinalabdin, D. M., Fadl, A., Ali, M. A., & Altayb, H. N. (2021). Helicobacter pylori 23S rRNA gene A2142G, A2143G, T2182C, and C2195T mutations associated with clarithromycin resistance detected in Sudanese patients. *BMC microbiology*, *21*(1), 38.

Acknowledgements:
The authors thank T*yi*DE-Toronto, Canada for helping to write this manuscript.

Funding:
The authors thank TCABS-E, Rajahmundry, India and T*yi*DE-Toronto, Canada for financial support.

Conflict of interest: This research article is an ongoing project currently at TCABS-E, Rajahmundry, India.

TCABSE-J Mini-Research Article
ISSN: 2583- 2557, *Volume 1, Issue 4, pp35-40. 2022.*

TCABSE-J
Interdisciplinary Sciences Journal

Survey of the janus kinase-1 (JAK-1) transcript variants and protein isoforms of JAK-1 to determine its druggability for acute lymphoid leukemia treatment.

[1, 2]Ramani S. Thokala & [1, 3]Ravikiran S. Yedidi*

[1]The Center for Advanced-Applied Biological Sciences & Entrepreneurship (TCABS-E), Visakhapatnam 530016, AP; [2]Department of Biotechnology and [3]Department of Zoology, Andhra University, Visakhapatnam 530003, AP. (*Correspondence to RSY: tcabse.india@gmail.com).

Acute lymphoblastic leukemia (ALL) has been one the major childhood cancers across the world causing high morbidity including in adults. The precursor lymphoblasts of both B- and T-cell lines developing into leukemia due to abnormal gene fusions has been well established by various research groups. Among the non-receptor tyrosine kinases that are responsible for ALL, the janus kinase-1 (JAK-1) has been implicated due to amino acid substitutions. Especially, the V658F mutation in JAK-1 is one of the most commonly observed amino acid substitutions in clinical samples of ALL. In this study the mutant JAK-1 (V658F) has been chosen for detailed analysis on its druggability. Our results suggest that the mutation containing flap/loop of JAK-1 has a 3.1 Å deviation in the C-alpha atoms of Val658 (wild type) and Phe658 (mutant). This structural deviation gives us enough selectivity for designing small molecule inhibitors that would specifically target only the mutant form of JAK-1 sparing the wild type as a potential therapeutic approach for ALL treatment. The V658F mutant JAK-1 inhibitor is currently under evaluation for future testing.

Keywords: Acute lymphoblastic leukemia, janus kinase-1, JAK1, clinical mutation, tyrosine kinase, kinase inhibitors, microRNA therapeutics.

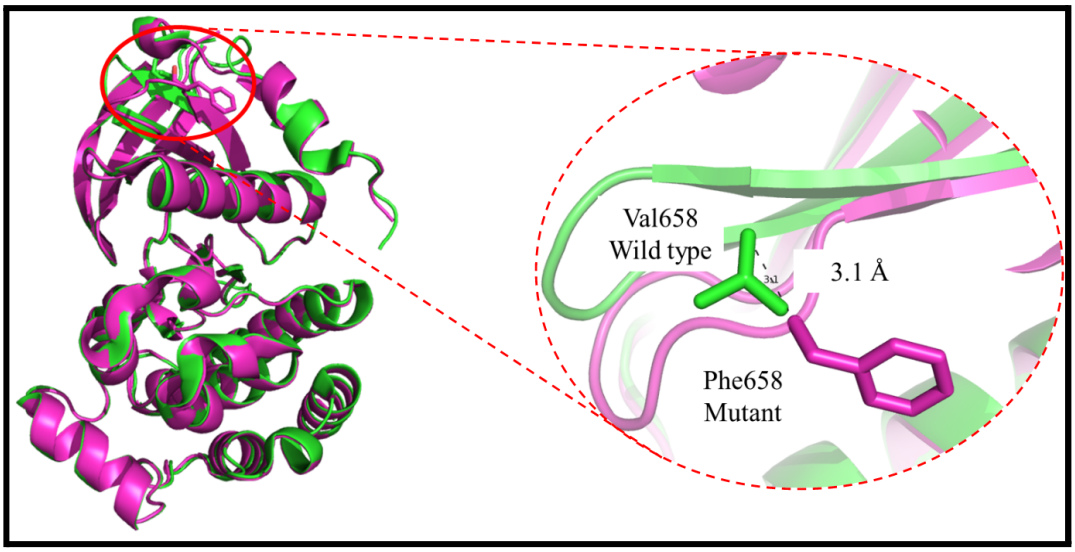

Figure 1. Conformational differences between the wild type and the V658F mutant of JAK1 provide selectivity for designing small molecule inhibitors that target the mutant form sparing the wild type.

Citation: Thokala, R. S. and Yedidi, R. S. (2022). Survey of the janus kinase-1 (JAK-1) transcript variants and protein isoforms of JAK-1 to determine its druggability for acute lymphoid leukemia treatment. *TCABSE-J*, Vol. 1, Issue 4: 35-40. Epub: Oct 5th, 2022.

TCABSE-J Mini-Research Article
ISSN: 2583- 2557, *Volume 1, Issue 4, pp35-40. 2022.*

Leukemia is a type of blood cancer in the bone marrow that results in the production of a high number of abnormal blood cells called blasts or leukemia cells. Some symptoms include bleeding and bruising, bone pain, fatigue and fever and these symptoms mainly occur due to lack of normal blood cells.In general diagnosis is usually done either by blood tests or bone marrow biopsy [1, 2]. The exact cause of leukemia is unknown [3]. Combination of some genetic factors and environmental factors are believed to play a role in causing leukemia [4, 5]. Risk factors mainly include smoking, radiation, chemicals and also prior chemotherapy. People with a family history of leukemia are at a higher risk. There are four main types of leukemia which include: acute lymphoblastic leukemia (ALL), acute myeloid leukemia (AML), chronic lymphocytic leukemia (CLL) and chronic myeloid leukemia (CML). Leukemias and lymphomas both belong to a broader group of tumors that affect the blood, bone marrow which are known as tumors of the hematopoietic and lymphoid tissues [6, 7]. Treatment involves chemotherapy, radiation therapy, targeted therapy, and bone marrow transplant. In addition to these, supportive care is needed. The success rate of treatment depends upon the type of leukemia and also the age of the person. The survival rate for a five-year old is 57% in the United States. In children under 15, the five-year old survival rate is greater than 60% or even about 90%, depending upon the type of leukemia. In children with acute leukemia who are cancer-free after five years, there is a chance of cancer likely to return [8].

In 2015, leukemia was present in almost 2.3 million people worldwide and caused nearly 353,500 deaths [9, 10]. It is the most common type of cancer in children, about three-quarters of leukemia cases in children are of acute lymphoblastic type. However, about 90% of all leukemias are diagnosed in adults, with CLL and AML and it is most common in adults [11]. Clinically, leukemia is subdivided into a large variety of groups. Generally they are classified into acute and chronic types [12].

ALL is a cancer of the lymphoid line of blood cells characterized by the development of large numbers of immature lymphocytes. Symptoms mainly include tiredness, pale skin color, fever, easy bleeding or bruising, enlarged lymph nodes, or sometimes even leads to bone pain. In acute leukemia, ALL increases rapidly and slowly becomes fatal within weeks or months if it is left untreated [13]. In most cases, the cause for acute lymphoblastic leukemia is unknown. Genetic risk factors may include Down syndrome, Li-Fraumeni syndrome. Environmental risk factors may include significant radiation exposure or prior chemotherapy. The mechanism involves multiple genetic mutations which results in rapid cell division. The excessive immature lymphocytes in the bone marrow interfere with the production of new red blood cells, white blood cells, and platelets. Diagnosis is generally based upon blood tests and bone marrow examination [14]. ALL is typically treated initially with chemotherapy is aimed at bringing about remission.Which is further followed by chemotherapy over a number of years. Treatment usually includes intrathecal chemotherapy since systemic chemotherapy can have limited penetration into the central nervous system as the central nervous system is a common site for the relapse of acute lymphoblastic leukemia. Treatment includes radiation therapy if spread to the brain, Stem cell transplantation may be used if the disease reoccurs then we need to follow the standard treatment [15]. Additional treatments such as Chimeric antigen receptor T (CAR-T) cell immunotherapy are also in use.

Janus kinase (JAK) is a family of intracellular, non-receptor tyrosine kinases (120-140 kDa) that transduce cytokine-mediated signals via the JAK-STAT pathway [16]. Janus kinase consists of two domains in which one domain exhibits the kinase activity, while the other domain negatively regulates the kinase activity of the first [17]. The four JAK family members are:

JAK-1, 2, 3 and Tyrosine kinase-2 (TYK-2). The JAK autophosphorylation induces a conformational change within itself, enabling it to transduce the intracellular signal by further phosphorylating and activating transcription factors called STATs (Signal Transducer and Activator of Transcription, or Signal Transduction And Transcription). The activated STATs dissociate from the receptor and form dimers before translocating to the cell nucleus, where they regulate transcription of selected genes [18]. Disrupted JAK-STAT signaling may lead to a variety of diseases, such as skin conditions, cancers, and disorders affecting the immune system [19-28]. JAK inhibitors (tofacitinib, baricitinib, upadacitinib and filgotinib) are used in the treatment of atopic dermatitis, rheumatoid arthritis, psoriasis, polycythemia vera, alopecia, essential thrombocythemia, ulcerative colitis, myeloid metaplasia with myelofibrosis and vitiligo [29-31].

In this study, we performed an extensive Bioinformatics and Computational survey of all the transcript variants of JAK-1 gene and the 3-dimensional structural analysis, respectively with a goal to target all the variants with a single small molecule inhibitor with reasonable selectivity and possibly lowest side effects. This potential therapeutic approach may result in new drugs for ALL treatment in the future.

Materials & Methods:

NCBI search & sequence alignment: The nucleotide sequences of 8 JAK-1 variants were searched for using NCBI RefSeq. The FASTA sequences of all the 8 variants were then aligned against each other using the Clustal Omega server in order to understand the length and conserved domains within these sequences. This multiple sequence alignment gives us an understanding about how all the 8 variants were differentially spliced.

Computing the RNA secondary structure: RNAfold web server will predict secondary structures of single stranded RNA or DNA sequences. The FASTA sequences were pasted into the box in order to build the secondary structures.

Secondary structure analysis of protein: The 3-D models for the two JAK-1 isoforms were built by using the SWISS MODEL server. These models were then downloaded and analyzed using PyMOL.

Results and Discussion:

NCBI search revealed 8 variants of JAK-1: The RefSeqGene for human JAK-1 with accession no: NG_023402.2 was taken as the original gene sequence that is unspliced in order to understand the full length of the gene. The full length gene contains 2,41,524 base pairs and is located on chromosome number 1. A search was performed using NCBI databases such as Gene and Nucleotide, which resulted in a list of 8 variants of JAK-1. Variants 4 and 5 are the longest (Table 1). These 8 variants were further sequence aligned using Clustal omega server.

NCBI Accession Number	Length (bp)
NM_002227.4	5,092
NM_001320923.2	5,015
NM_001321852.2	5,018
NM_001321853.2	5,277
NM_001321854.2	5,193
NM_001321855.2	5,176
NM_001321856.2	4,931
NM_001321857.2	5,089

Table 1. List of 8 JAK-1 transcript variants from NCBI.

```
NP_001308785.1: MQYLNIKEDCNAMAFCAKMRSSKKTEVNLEAPEPGVEVIFYLSDREPLRLGSGEYTAEELCIRAAQACRISPLCH   75
NP_001308786.1: MQYLNIKEDCNAMAFCAKMRSSKKTEVNLEAPEPGVEVIFYLSDREPLRLGSGEYTAEELCIRAAQACRISPLCH   75
                ********************************************************************************

NP_001308785.1: NLFALYDENTKLWYAPNRTITVDDKMSLRLHYRMRFYFTNWHGTNDNEQSVWRHSPKKQKNGYEKKKIPDATPLL  150
NP_001308786.1: NLFALYDENTKLWYAPNRTITVDDKMSLRLHYRMRFYFTNWHGTNDNEQSVWRHSPKKQKNGYEKKKIPDATPLL  150
                ********************************************************************************

NP_001308785.1: DASSLEYLFAQGQYDLVKCLAPIRDPKTEQDGHDIENECLGMAVLAISHYAMMKKMQLPELPKDISYKRYIPETL  225
NP_001308786.1: DASSLEYLFAQGQYDLVKCLAPIRDPKTEQDGHDIENECLGMAVLAISHYAMMKKMQLPELPKDISYKRYIPETL  225
                ********************************************************************************

NP_001308785.1: NKSIRQRNLLTRMRINNVFKDFLKEFNNKTICDSSVSTHDLKVKYLATLETLTKHYGAEIFETSMLLISSENEMN  300
NP_001308786.1: NKSIRQRNLLTRMRINNVFKDFLKEFNNKTICDSSVSTHDLKVKYLATLETLTKHYGAEIFETSMLLISSENEMN  300
                ********************************************************************************

NP_001308785.1: WFHSNDGGNVLYYEVMVTGNLGIQWRHKPNVVSVEKEKNKLKRKKLENKHKKDEEKNKIREEWNNFSYFPEITHI  375
NP_001308786.1: WFHSNDGGNVLYYEVMVTGNLGIQWRHKPNVVSVEKEKNKLKRKKLENKHKKDEEKNKIREEWNNFSYFPEITHI  375
                ********************************************************************************

NP_001308785.1: VIKESVVSINKQDNKKMELKLSSHEEALSFVSLVDGYFRLTADAHHYLCTDVAPPLIVHNIQNGCHGPICTEYAI  450
NP_001308786.1: VIKESVVSINKQDNKKMELKLSSHEEALSFVSLVDGYFRLTADAHHYLCTDVAPPLIVHNIQNGCHGPICTEYAI  450
                ********************************************************************************

NP_001308785.1: NKLRQEGSEEGMYVLRWSCTDFDNILMTVTCFEKSEQVQGAQKQFKNFQIEVQKGRYSLHGSDRSFPSLGDLMSH  525
NP_001308786.1: NKLRQEGSEEGMYVLRWSCTDFDNILMTVTCFEKSE-VQGAQKQFKNFQIEVQKGRYSLHGSDRSFPSLGDLMSH  524
                ************************************ ************************************

NP_001308785.1: LKKQILRTDNISFMLKRCCQPKPREISNLLVATKKAQEWQPVYPMSQLSFDRILKKDLVQGEHLGRGTRTHIYSG  600
NP_001308786.1: LKKQILRTDNISFMLKRCCQPKPREISNLLVATKKAQEWQPVYPMSQLSFDRILKKDLVQGEHLGRGTRTHIYSG  599
                ********************************************************************************

NP_001308785.1: TLMDYKDDEGTSEEKKIKVILKVLDPSHRDISLAFFEAASMMRQVSHKHIVYLYGVCVRDVENIMVEEFVEGGPL  675
NP_001308786.1: TLMDYKDDEGTSEEKKIKVILKVLDPSHRDISLAFFEAASMMRQVSHKHIVYLYGVCVRDVENIMVEEFVEGGPL  674
                ********************************************************************************

NP_001308785.1: DLFMHRKSDVLTTPWKFKVAKQLASALSYLEDKDLVHGNVCTKNLLLAREGIDSECGPFIKLSDPGIPITVLSRQ  750
NP_001308786.1: DLFMHRKSDVLTTPWKFKVAKQLASALSYLEDKDLVHGNVCTKNLLLAREGIDSECGPFIKLSDPGIPITVLSRQ  749
                ********************************************************************************

NP_001308785.1: ECIERIPWIAPECVEDSKNLSVAADKWSFGTTLWEICYNGEIPLKDKTLIEKERFYESRCRPVTPSCKELADLMT  825
NP_001308786.1: ECIERIPWIAPECVEDSKNLSVAADKWSFGTTLWEICYNGEIPLKDKTLIEKERFYESRCRPVTPSCKELADLMT  825
                ********************************************************************************

NP_001308785.1: RCMNYDPNQRPFFRAIMRDINKLEEQNPDIVSEKKPATEVDPTHFEKRFLKRIRDLGEGHFGKVELCRYDPEGDN  900
NP_001308786.1: RCMNYDPNQRPFFRAIMRDINKLEEQNPDIVSEKKPATEVDPTHFEKRFLKRIRDLGEGHFGKVELCRYDPEGDN  899
                ********************************************************************************

NP_001308785.1: TGEQVAVKSLKPESGGNHIADLKKEIEILRNLYHENIVKYKGICTEDGGNGIKLIMEFLPSGSLKEYLPKNKNKI  975
NP_001308786.1: TGEQVAVKSLKPESGGNHIADLKKEIEILRNLYHENIVKYKGICTEDGGNGIKLIMEFLPSGSLKEYLPKNKNKI  974
                ********************************************************************************

NP_001308785.1: NLKQQLKYAVQICKGMDYLGSRQYVHRDLAARNVLVESEHQVKIGDFGLTKAIETDKEYYTVKDDRDSPVFWYAP 1050
NP_001308786.1: NLKQQLKYAVQICKGMDYLGSRQYVHRDLAARNVLVESEHQVKIGDFGLTKAIETDKEYYTVKDDRDSPVFWYAP 1049
                ********************************************************************************
NP_001308785.1: ECLMQSKFYIASDVWSFGVTLHELLTYCDSDSSPMALFLKMIGPTHGQMTVTRLVNTLKEGKRLPCPPNCPDEVY 1125
NP_001308786.1: ECLMQSKFYIASDVWSFGVTLHELLTYCDSDSSPMALFLKMIGPTHGQMTVTRLVNTLKEGKRLPCPPNCPDEVY 1124
                ********************************************************************************

NP_001308785.1: QLMRKCWEFQPSNRTSFQNLIEGFEALLK 1154
NP_001308786.1: QLMRKCWEFQPSNRTSFQNLIEGFEALLK 1153
                ****************************
```

Figure 2. Clustal omega alignment of JAK-1 isoforms.

Multiple sequence alignment of JAK-1 mRNA transcript variants: The nucleotide sequences of all 8 JAK-1 variants were aligned against each other using the CLUSTAL-OMEGA server in order to understand the length and conserved domains within these sequences. Variants 4 and 5 are the longest (Table 1) and showed proper alignment from the 5'-end to the 3'-end while the other variants were not properly aligned at the 5'-end but were absolutely aligned at the 3'-end. This multiple sequence alignment gives us an understanding about how the 8 variants were differentially spliced post-transcription.

Variant	MFE (kcal/mol.)	Diversity
1	-1608.32	1340.92
2	-1533.00	1368.23
3	-1534.05	1231.20
4	-1655.12	1304.88
5	-1627.81	1536.48
6	-1629.69	1187.29
7	-1514.48	1357.97
8	-1602.21	1337.11

Table 2. Mean free energy (MFE) values of variant mRNAs.

Secondary structure analysis of mRNA transcript variants of JAK-1: The secondary structure analysis of all the 8 mRNA transcript variants of JAK-1 was performed to understand their structural diversity as well as their stability. As shown in Table 2, the thermodynamic minimum free energy values of each variant along with their corresponding ensemble diversity values were compared and analyzed. Among the 8 variants, variant 4 shows higher stability relatively and variant 7 shows the least stability relatively with an energy difference of 141 kcal/mol. between the two variants. Based on our studies in this article, we conclude that all the 8 mRNA transcript variants of JAK-1 possess similar profiles of stability and the two protein isoforms have more than 99% amino acid sequence homology. However, the structural analysis of wild type vs. the V658F mutant of JAK-1 confirmed that the structural deviation of 3.1 Å can be leveraged for the design of selective inhibitors that bind to the V658F mutant form of JAK-1 sparing the wild type. It is noteworthy to mention that the selective inhibitors will only work if the patient is heterozygous for mutant JAK-1 so that if the mutant form is inhibited, the wild type can function. On the other hand, if the patient is homozygous for mutation, then the inhibitor may not work as expected. Currently we are in the process of synthesizing a library of analogs based on a lead molecule that was identified *in silico*. The structure-activity relationship studies in this regards will be published in the future issues of TCABSE-J.

References

1. Devine SM, Larson RA. Acute leukemia in adults: recent developments in diagnosis and treatment. CA Cancer J Clin. 1994 Nov-Dec;44(6):326-52. doi: 10.3322/canjclin.44.6.326. PMID: 7953914.
2. "What You Need To Know About™ Leukemia". *National Cancer Institute*. 23 December 2013. Archived from the original on 6 July 2014. Retrieved 18 June 2014.
3. Hutter, JJ (June 2010). "Childhood leukemia". *Pediatrics in Review*. 31 (6): 234–41. doi:10.1542/pir.31-6-234. PMID 20516235.
4. "A Snapshot of Leukemia". *NCI*. Archived from the original on 4 July 2014. Retrieved 18 June 2014.
5. Cordo V, Meijerink J (January 2021). "T-cell Acute Lymphoblastic Leukemia: A Roadmap to Targeted Therapies". *Blood Cancer Discovery*. 2: 19–31. doi:10.1158/2643-3230.BCD-20-0093. ISSN 2643-3230. PMC 8447273.
6. Vardiman, JW; Thiele, J; Arber, DA; Brunning, RD; Borowitz, MJ; Porwit, A; Harris, NL; Le Beau, MM; Hellström-Lindberg, E; Tefferi, A; Bloomfield, CD (30 July 2009). "The 2008 revision of the World Health Organization (WHO) classification of myeloid neoplasms and acute leukemia: rationale and important changes". *Blood*. 114 (5): 937–51. doi:10.1182/blood-2009-03-209262. PMID 19357394. S2CID 3101472.
7. Cătoi, Alecsandru Ioan Baba, Cornel (2007). *Comparative oncology*. Bucharest: The Publishing House of the Romanian

Academy. p. Chapter 17. ISBN 978-973-27-1457-7. Archived from the original on 10 September 2017.
8. American Cancer Society (2 March 2014). "Survival rates for childhood leukemia". Archived from the original on 14 July 2014.
9. GBD 2015 Disease and Injury Incidence and Prevalence, Collaborators. (8 October 2016). "Global, regional, and national incidence, prevalence, and years lived with disability for 310 diseases and injuries, 1990–2015: a systematic analysis for the Global Burden of Disease Study 2015". *Lancet*. 388 (10053): 1545–1602.
10. GBD 2015 Mortality and Causes of Death, Collaborators. (8 October 2016). "Global, regional, and national life expectancy, all-cause mortality, and cause-specific mortality for 249 causes of death, 1980–2015: a systematic analysis for the Global Burden of Disease Study 2015". *Lancet*. 388 (10053): 1459–1544.
11. *World Cancer Report 2014*. World Health Organization. 2014. pp. Chapter 5.13. ISBN 978-9283204299
12. "Questions and Answers About Leukemia" (PDF). *Center for Disease Control and Prevention*. Archived (PDF) from the original on 30 July 2021. Retrieved 8 August 2021.
13. Marino BS, Fine KS (2013). *Blueprints Pediatrics*. Lippincott Williams & Wilkins. p. 205. ISBN 9781451116045.
14. Ferri, Fred F. (2017). *Ferri's Clinical Advisor 2018 E-Book: 5 Books in 1*. Elsevier Health Sciences. p. 743. ISBN 9780323529570.
15. Hunger SP, Mullighan CG (October 2015). "Acute Lymphoblastic Leukemia in Children". *The New England Journal of Medicine*. 373 (16): 1541–52.
16. Rodig SJ, Meraz MA, White JM, Lampe PA, Riley JK, Arthur CD, King KL, Sheehan KC, Yin L, Pennica D, Johnson EM, Schreiber RD (1998). "Disruption of the Jak1 gene demonstrates obligatory and nonredundant roles of the Jaks in cytokine -induced biologic responses". *Cell*. 93 (3): 373–83.
17. Kisseleva; Bhattacharya, S; Braunstein, J; Schindler, CW; et al. (2002-02-20). "Signaling through the JAK/STAT pathway, recent advances and future challenges". *Gene*. 285 (1–2): 1–24.
18. Kisseleva; Bhattacharya, S; Braunstein, J; Schindler, CW; et al. (2002-02-20). "Signaling through the JAK/STAT pathway, recent advances and future challenges". *Gene*. 285 (1–2): 1–24.
19. Aaronson DS, Horvath CM (2002). "A road map for those who don't know JAK-STAT". *Science*. 296 (5573): 1653–5. Bibcode:2002Sci...296.1653A.
20. Jatiani, S. S.; Baker, S. J.; Silverman, L. R.; Reddy, E. P. (2011). "JAK/STAT Pathways in Cytokine Signaling and Myeloproli -ferative Disorders: Approaches for Targeted Therapies". *Genes & Cancer*. 1 (10): 979–993.
21. Freund, P.; Kerenyi, M. A.; Hager, M.; Wagner, T.; Wingelhofer, B.; Pham, H T T.; Elabd, M.; Han, X.; Valent, P.; Gouilleux, F.; Sexl, V.; Krämer, O. H.; Groner, B.; Moriggl, R. (2017). "O-GlcNAcylation of STAT5 controls tyrosine phosphorylation and oncogenic transcription in STAT5-dependent malignancies". *Leukemia*. 31 (10): 2132–2142.
22. Schindler, Christian; Levy, David E.; Decker, Thomas (2007). "JAK-STAT Signaling: From Interferons to Cytokines". *Journal of Biological Chemistry*. 282 (28): 20059–20063.
23. Aaronson DS, Horvath CM (2002). "A road map for those who don't know JAK-STAT". *Science*. 296 (5573): 1653–5. Bibcode:2002Sci...296.1653A.
24. Kiu, Hiu; Nicholson, Sandra E. (2012). "Biology and significance of the JAK/STAT signaling pathways". *Growth Factors*. 30(2): 88–106.
25. Reich, Nancy C; Rout, M. P. (2014). "STATs get their move on". *JAK-STAT*. 2 (4): 27080.
26. Liu, L.; McBride, K. M.; Reich, N. C. (2005). "STAT3 nuclear import is independent of tyrosine phosphorylation and mediated by importin- 3". *Proceedings of the National Academy of Sciences*. 102 (23): 8150–8155.
27. Flex E *et al*. Somatically acquired JAK1 mutations in adult acute lymphoblastic leukemia. J Exp Med. 2008 Apr 14;205(4):751-8.
28. Eun Goo Jeong, Min Sung Kim, Hyo Kyung Nam, Chang Ki Min, Seok Lee, Yeun Jun Chung, Nam Jin Yoo and Sug Hyung Lee. Somatic Mutations of *JAK1* and *JAK3* in Acute Leukemias and Solid Cancers. Clin Cancer Res June 15 2008 (14) (12) 3716-3721.
29. "Search for: GLPG0634 - List Results - ClinicalTrials.gov". *clinicaltrials.gov.*
30. Principles of Pharmacology: The Pathophysiologic Basis of Drug Therapy: D. Golan et al. LWW. 2007.
31. Craiglow, B. G.; King, B. A. (2015). "Tofacitinib Citrate for the Treatment of Vitiligo: A Pathogenesis-Directed Therapy". *JAMA Dermatology*. 151(10): 1110–2.

Acknowledgements:
The authors thank T*yi*DE-Toronto, Canada for helping to write this manuscript.

Funding:
The authors thank TCABS-E, Rajahmundry, India and T*yi*DE-Toronto, Canada for financial support.

Conflict of interest:
This research article is an ongoing project currently at TCABS-E, Rajahmundry, India. However the authors welcome academic collaborations from various groups.

TCABSE-J Application Reports
ISSN: 2583- 2557, *Volume 1, Issue 4, pp 42-45. 2022.*

TCABSE-J
Interdisciplinary Sciences Journal

Design of a minimally invasive stem cell therapy by targeted sonic hedgehog protein engineering for intervertebral disc damage repair.

[1]Devi Lakshmi P. Korangi and [1, 2]Ravikiran S. Yedidi*

[1]The Center for Advanced-Applied Biological Sciences & Entrepreneurship (TCABS-E), Rajahmundry, AP, India; [2]Department of Zoology, Andhra University, Visakhapatnam, AP, India.
(*Correspondence to RSY: tcabse.india@gmail.com).

Spinal cord injury leading to the intervertebral disc [IVD] damage leads to chronic pain and requires surgery with long recovery times. At present, pain management and post surgical physiotherapy are available as options. The long process of healing severely affects the patient's life in different ways. In order to cut down the healing time with the same results we hypothesized that one can genetically program stem cells into IVD producing progenitor cells and deliver them precisely to the site of injury to naturally recover from the damaged IVDs. This method is minimally invasive compared to complex surgery. In this study, the sonic hedgehog [SHH] protein was chosen as the target for genetic engineering to differentiate the stem cells *in vitro* before using them for IVD damage repair. SHH plays a critical role in cell differentiation. We performed a detailed structural analysis of SHH bound to the patched receptor for protein engineering and chemical biology approaches.

Keywords: Stem cells, spinal disc damage, genetic engineering, sonic hedgehog gene, therapy.

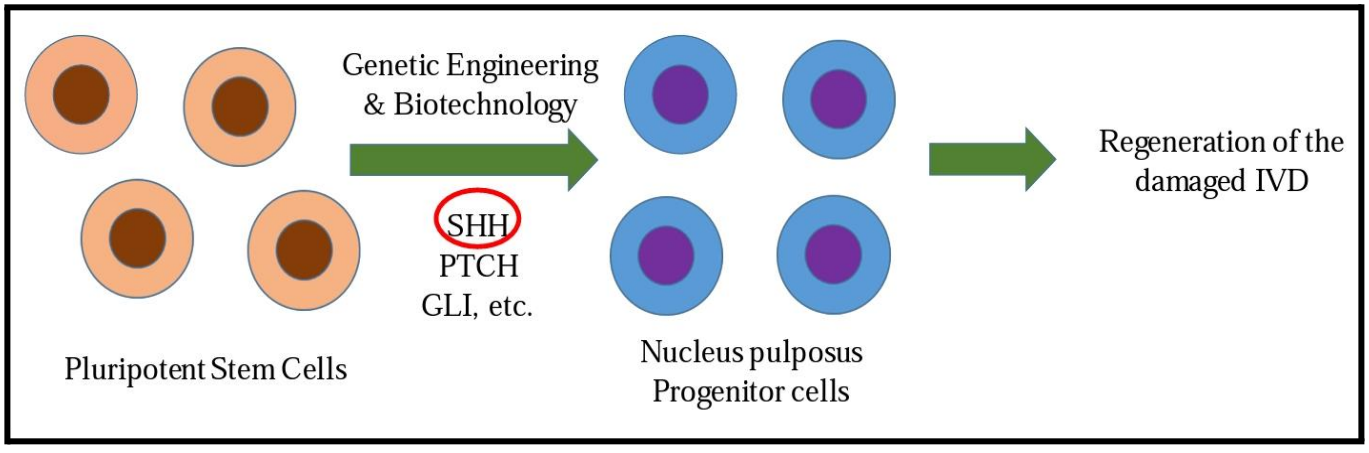

Figure 1. The overall proposed workflow for stem cell therapy treatment to repair the damaged IVDs using genetic engineering and protein engineering protocols.

Citation: Korangi, D. P. and Yedidi, R.S. (2022). Design of a minimally invasive stem cell therapy by targeted sonic hedgehog protein engineering for intervertebral disc damage repair. *TCABSE-J*, Vol. 1, Issue 4: 41-44. Epub: Oct5th, 2022.

Among the major disorders, intervertebral disc (IVD) damage has been a menace throughout the world. Majority of the adults aged 30-50 are affected by IVD damage. IVD is mostly caused due to heavy weight lifting and working continuously for long hours. Human spine is made up of 33 bones called vertebrae. IVD is the disc that is present in between the two vertebrae of the spinal cord except for the first cervical segment. There are 23 discs in the human spine (6-cervical region, 12-thoracic region, 5-lumbar region). Each disc contains a nucleus that acts as a shock absorber, absorbing the impact of the body's activity and keeps the two vertebrates separately acting as strong elastic pivot for each joint segment of the spine. Disc has a tough exterior with a soft, gel-like interior creating cushions between the bones. Each Disc is covered on the two sides by the subchondral plate and cartilaginous endplate. The nucleus consists of nucleus pulposus and the outer region comprises of annulus fibrosus. Nearly 60-80% of the disc consists of water and the remaining primarily consists of type - 2 collagen and proteoglycans.

The common type of disc problem includes, (i) Herniated disc or slipped disc, (ii) Pinched nerve, (iii) Degenerative disc disease, (iv) Spinal stenosis, (v) Sciatica and (vi) Bulging disc. Common symptoms of the IVD damage problem include back pain, arm pain, neck pain, leg pain, muscle weakness, numbness, burning difficulty in walking and sleeping. The available treatment options for these problems are hot cold therapy, physical therapy, steroid injections, yoga, acupuncture, chiropractic manipulations and massage therapy. In severe cases surgery is performed. But these treatment options don't ensure complete cure.

In this study, we hypothesized that one can genetically program pluripotent stem cells into Nucleus pulposus progenitor cells and deliver them precisely to the site of injury to naturally recover from the damaged IVDs (Figure 1). We propose to use the pluripotent stem cells from bone marrow or umbilical cord as a starting point and genetically engineer them into nucleus pulposus progenitor cells that can naturally regenerate the damaged IVD. As a part of the proposed genetic engineering protocol, we are focussing on the sonic hedgehog (SHH) pathway first which interacts with cell receptor proteins such as patched [PTCH] and transcription factors such as gli. SHH is a growth factor protein responsible for cell differentiation during embryonic development. SHH interacts with patched (PTCH) and smoothened (SMO) receptors and triggers the downstream signals. Gli is a transcription factor that relocates into the nucleus and helps the expression of SHH target genes which further help in cellular differentiation. The activation of SHH signaling requires binding of SHH to the PTCH mediated smoothened (SMO) (PTCH-SMO) receptor complex and induction of downstream signaling cascade. This is a heterodimeric receptor complex consisting of two transmembrane subunits, namely PTCH and SMO. They have seven alpha helices that play a major role in the downstream SHH signaling. The PTCH suppressor is normally a molecular transporter. PTCH indirectly inhibits the SMO activity as a response to the binding of SHH with PTCH. SMO is activated and stabilized. The activated SMO initiates the SHH downstream signaling cascade. It generates intracellular signals that regulate several protein kinases, which activates transcription factors such as GLI.

In order to understand the overall organization of the SHH analysis of its core domain structure was performed using computational biology tools. Structure of SHH was downloaded from the protein data bank (PDB ID: 3HO5). The analysis includes evaluation of structure (α helices and β strands) using PyMOL molecular graphics software. Hydrogen bond analysis was performed using PyMOL. All hydrogen bonds with bond lengths less than 3 Å were considered as strong hydrogen bonds (Table 1). Evidently, only 4 out of 13 hydrogen bonds were found to be weaker.

TCABSE-J Application Reports
ISSN: 2583- 2557, *Volume 1, Issue 4, pp 42-45. 2022.*

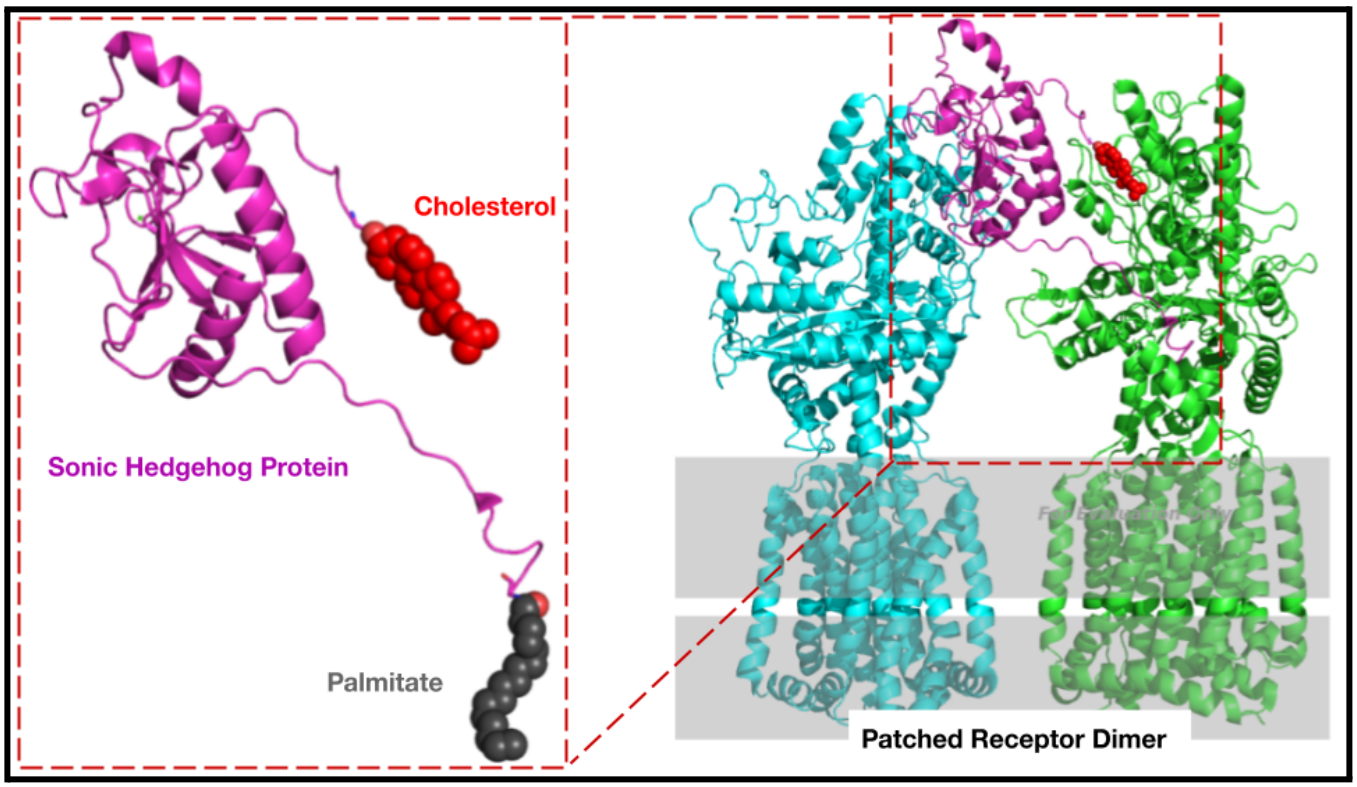

Figure 2. Structure of SHH and PTCH dimer.

SHH is a 45 kilo Dalton protein containing 462 amino acids. SHH consists of an N-terminal and a C-terminal domain with a protease cleavage site in between. After cleavage, the N-terminal domain binds palmitate and cholesterol to become functionally active. Next, we analyzed the binding interactions of SHH with PTCH (PDB ID: 6RVD). The right panel of Figure 2 shows the active complex in which the SHH is bound to PTCH such that the smoothened (SMO) allows the transcription of target genes through GLI1 but when the hedgehog interacting protein (HHIP) binds to SHH then SMO is inhibited so that the downstream transcription of the target genes is also inhibited. The current study revealed the interactions between SHH and HHIP (PDB ID: 3HO5) shedding light on how SHH is regulated by the HHIP from binding PTCH. This mechanism of SHH targeted gene regulation can be achieved by tweaking the interactions between SHH and HHIP to enhance their mutual binding affinities.

SHH	Bond length	HHIP
Tyr44	2.7A	Thr418
Tyr44	2.6A	Asp387
Lys178	3.4A	Asp387
Glu176	2.6A	Gly384
His180	2.9A	Asp383
Glu136	3.0A	Ala311
His133	3.4A	Asp383
Arg153	2.9A	Glu380
Arg153	3.0A	Glu380
Arg123	3.1A	Glu380
Lys87	2.8A	Glu380
Lys87	2.8A	Glu381
Thr125	3.1A	Glu380

Table 1. List of hydrogen bonds between SHH and HHIP.

This strategy will be used as a part of our protein engineering protocol that will be used in future to differentiate stem cells into nucleus pulposus progenitor cells. These differentiated cells will then be tested in animals for their performance in the IVD damage repair. All further research on this project will be published in the future issues of TCABSE-J.

References

1. Pattappa, G., Li, Z., Peroglio, M., Wismer, N., Alini, M., & Grad, S. (2012). Diversity of intervertebral disc cells: phenotype and function. *Journal of anatomy*, *221*(6), 480–496.
2. Sakurai, H., Sakaguchi, Y., Shoji, E., Nishino, T., Maki, I., Sakai, H., Hanaoka, K., Kakizuka, A., & Sehara-Fujisawa, A. (2012). In vitro modeling of paraxial mesodermal progenitors derived from induced pluripotent stem cells. *PloS one*, *7*(10), e47078.
3. Borycki, A. G., Mendham, L., & Emerson, C. P., Jr (1998). Control of somite patterning by Sonic hedgehog and its downstream signal response genes. *Development (Cambridge, England)*, *125*(4), 777–790.
4. Tendulkar, G., Chen, T., Ehnert, S., Kaps, H. P., & Nüssler, A. K. (2019). Intervertebral Disc Nucleus Repair: Hype or Hope?. *International journal of molecular sciences*, *20*(15), 3622.
5. Fontes, A., Macarthur, C. C., Lieu, P. T., & Vemuri, M. C. (2013). Generation of human-induced pluripotent stem cells (hiPSCs) using episomal vectors on defined Essential 8™ Medium conditions. *Methods in molecular biology (Clifton, N.J.)*, *997*, 57–72.
6. Tang, R., Jing, L., Willard, V. P., Wu, C. L., Guilak, F., Chen, J., & Setton, L. A. (2018). Differentiation of human induced pluripotent stem cells into nucleus pulposus-like cells. *Stem cell research & therapy*, *9*(1), 61.
7. Oh, J., Lee, K. I., Kim, H. T., You, Y., Yoon, D. H., Song, K. Y., Cheong, E., Ha, Y., & Hwang, D. Y. (2015). Human-induced pluripotent stem cells generated from intervertebral disc cells improve neurologic functions in spinal cord injury. *Stem cell research & therapy*, *6*(1), 125.
8. Choi, H., Johnson, Z. I., & Risbud, M. V. (2015). Understanding nucleus pulposus cell phenotype: a prerequisite for stem cell based therapies to treat intervertebral disc degeneration. *Current stem cell research & therapy*, *10*(4), 307–316.
9. Bosanac, I., Maun, H., Scales, S. *et al.* The structure of SHH in complex with HHIP reveals a recognition role for the Shh pseudo active site in signaling. *Nat Struct Mol Biol* 16, 691–697 (2009).

Acknowledgements: The authors thank T*yi*DE-Toronto, Canada for helping to write this manuscript.

Funding: The authors thank TCABS-E, Rajahmundry, India and TyiDE-Toronto, Canada for financial support.

Conflict of interest: The applications report presented here is a currently ongoing project at TCABS-E, Rajahmundry, India. The authors invite collaborations without any conflict of interest.

The Center for Advanced-Applied Biological Sciences & Entrepreneurship (TCABS-E)

Danavaipeta, Rajahmundry; Tel./WhatsApp: 8660301662; Email: tcabse.india@gmail.com

© All rights reserved.
Published by TCABS-E Press on behalf of TCABS-E, Rajamahendravaram. India.